Modeling and Simulation of 1^{st} Compression Ring Dynamics in High Torque Low-Speed Diesel Engine

JAMAL AHMED
00000119730

Supervisor
DR. RAJA AMER AZIM

DEPARTMENT OF MECHANICAL ENGINEERING
COLLEGE OF ELECTRICAL & MECHANICAL ENGINEERING
NATIONAL UNIVERSITY OF SCIENCES AND TECHNOLOGY
ISLAMABAD
AUGUST, 2019

Modeling and Simulation of 1^{st} Compression Ring Dynamics in High Torque Low Speed Diesel Engine

JAMAL AHMED

00000119730

A thesis submitted in partial fulfillment of the requirements for the degree of

MS Mechanical Engineering

Thesis Supervisor:

Dr. Raja Amer Azim

Thesis Supervisor's Signature:_____

DEPARTMENT OF MECHANICAL ENGINEERING

COLLEGE OF ELECTRICAL & MECHANICAL ENGINEERING

NATIONAL UNIVERSITY OF SCIENCES AND TECHNOLOGY, ISLAMABAD

AUGUST, 2019

Declaration

I certify that this research work titled "*Modeling and Simulation of* 1^{st} *Compression Ring Dynamics in High Torque Low-Speed Diesel Engine"* is my own work. The work has not been presented elsewhere for assessment. The material that has been used from other sources it has been properly acknowledged / referred.

Signature of Student

Jamal Ahmed

00000119730

Language Correctness Certificate

This thesis has been read by an English expert and is free of typing, syntax, semantic, grammatical and spelling mistakes. Thesis is also according to the format given by the university.

Signature of Student

Jamal Ahmed

00000119730

Signature of Supervisor

Dr. Raja Amer Azim

Copyright Statement

Acknowledgements

First and foremost, I would like to thank The Allah Almighty, Who lead this work to be completed in time and whose blessings and help kept me sheltered all the time.
I would like to thank to my departmental supervisor Dr. Raja Amer Azim; for his humble attitude and for all of his guidance throughout the difficult phases of my research work. I feel proud that I got the chance to work with such a noble person. Without his consistent guidance, this work may have not been accomplished.
I would like to say special thanks to my supervisor and my respectable teacher Dr. Syed Adnan Qasim .That was the turning point of my life when for the first time I met with him. He is a visionary person who gave me a true aim of my life. By his unique way of teaching style he made my knowledge base strong. During my research work, whenever I felt frustrated he always believed in me and kept me motivated throughout the research phase. Without his efforts, that was not possible for me to complete my research work.
I would like to thank my beloved parents who showed patience and whose consistent encouragement made it possible for me to achieve what I have today. I would not forget to say thank to my senior and respectable friend Mr. Saqib Naseer who remained a source of motivation throughout my research work. He always motivated me through every bad time during research work. Whenever I got disappointed and I discussed the matter with him, he was person who realized me to believe on my capabilities. I would like to say thank to Mr. Kishwat Ijaz Malik who was always available to provide technical insight in my research work. He taught me a lot of things which are necessary for research work.
.I would say thanks to my dear friend Mr. Waleed Hussain for spending a precious time during research work, whose was always available for me for any kind of help.
I would to thank to all the faculty members like Dr. Tariq Talha, Dr. Hassan Aftab Saeed, Dr. Saifullah Khalid and respectable staff at mechanical department for their cooperation and guidance.
I have been fortunate to meet and work with many wonderful people like Mr. Hussain Ahmed Tariq, Mr. Awais Ahmed, Mr. Ahsan Naseer who made my time at college enjoyable and whose continues encouragement made it possible for me to reach all the way to this point.
In the end ,I would like to thank the entire honorable faculty of mechanical department of the college, whose professional approach and vision groomed me.

To my beloved Parents, Teachers and Siblings…

Abstract

In this modern age , engine design requires improved fuel economy, reduction of exhaust carbon emissions, enhanced recyclability, increased operating life and freedom of generating hazardous substances. To meet these demands engine design manufacturers make it confirm that piston ring design must minimize the friction loss due to direct dry contact and lubricant internal resistance, oil consumption loss due oil transport to combustion chamber side, wear loss due to direct contact between ring and liner. Before mentioned requirements can be achieved if ring dynamics is properly implemented within groove. Proper selection of groove side clearance decreases the gas blow-by effect. Implementation of fully flooded conditions at inlet and outlet of region ring-liner interface develops hydrodynamic lubrication to avoid adhesive wear and dry contact. In the absence of fully flooded lubrication within the ring-liner interface increases the chance of dry contact within ring-liner interface which results in sequential change in lubrication regimes of boundary, mixed, hydrodynamic in a diesel engine. This sequential change in lubrication regimes prone to friction loss, power loss, hence enhanced the wear phenomenon. Studies have shown that cylinder is not in perfect circular shape due to mechanical loadings, thermal distortion, wear, high combustion gas pressure and manufacturing error. Distorted cylinder liner results in lower magnitude of minimum oil film thickness in circumferential cylinder side, which results in enhanced oil consumption due to oil transport to combustion chamber side and ultimately decreases overall power.

In this research work, ring dynamics in radial and axial direction, gas flow model and piston secondary motion was analyzed in high torque low speed diesel engine. Parametric study is conducted for clearance in radial direction, clearance in axial direction, engine speed and degree of distortion in non-circular cylinder liner. Results showed that gas flow rates are sensitive to ring groove clearances. It was also observed that piston tilt has crucial effects on oil film thickness and hydrodynamic pressure and ring hydrodynamic friction force. Results showed that parabolic ring running face profile is best suited for improved lubricating film thickness profile and performance. It was also observed that with increase in engine speed, film thickness profile improves and proper hydrodynamic regime developed. It was also noticed that oil film thickness and ring performance improved with an increase in magnitude of bore distortion. It was noticed that Increase in groove side clearance in axial direction enhance the gas blow-by effect from combustion side to crankcase side.

Table of Contents

List of Figures

List of Tables

CHAPTER 1

INTRODUCTION

1.1Aim of Research

Aim of the research is to incorporate the piston secondary motion effects on ring dynamics. In radial direction, hydrodynamic pressure will be estimated under hydrodynamic lubrication. These hydrodynamic pressure will define the ring radial motion in term of minimum oil film thickness. Ring axial motion will be considered when piston is taken in static position. Then it will be estimated how ring axial motion will affect the gas flow rate when ring transits between groove upper and lower flanks. Then piston lubrication phenomena will be considered. Piston secondary motions represented by its top eccentricity, bottom eccentricity and tilt motion will be investigated. Piston tilt impact on ring dynamics will be analyzed that how tilt motion effect the ring hydrodynamic pressure, minimum film thickness and hydrodynamic friction force.

1.2Background

The reliability and efficiency of heavy duty diesel engines have their massive use in this world. Based on engine different sizes heavy duty diesel engines are being used in industrial as well as in defense industry. These engines have high torque and low speed as compared to petrol engines. Due to good ratio of air fuel output power of these engines has improved referred as high torque engines. High torque diesel engines have many functions like in marine engines, cranes, road rollers, dumpers, bulldozers etc. In a diesel engine, piston assembly is important part to understand tribological behavior. Piston acts as sliding bearing and shows reciprocating motion which is called primary motion. Piston also shows two other motions in lateral direction which is due to clearance in radial direction perpendicular to cylinder surface and other is due to piston tilt in angular direction, this tilt motion is basically generated based on top and bottom eccentricity. Piston is actually is a long slider bearing and have mostly parabolic profile that is the reason it has two different piston top clearance and bottom side clearance. Piston lateral and tilt movements are results of imbalance of forces acting on piston surface during piston motion between TDC and BDC. In piston assembly major factor which involve measuring the performance of assembly parts such as friction losses, wear measurement, power losses are highly based on dynamics and lubrication. Radial clearance is also main contributor in all these losses due to small clearance in radial direction is a big cause of friction losses which ultimately enhance the power losses. Piston primary motion is reciprocating motion which is defined by it kinematic relation of displacement, velocity and acceleration. Rings are also important part of engine assembly. Ring are unlocked within respective grooves and show independent motions. According to specific function, normally three rings are used in piston assembly. Ring proper dynamics within groove is defined by ring radial motion, ring axial motion and ring angular motion. Understudy the focus will be on 1^{st} compression ring. 1^{st} Compression is fitted within 1 groove which is situated just below the combustion chamber. . 1^{st} Compression has two basic purposes, firstly, it seals the blow-by gases (burnt gases) trailing down from combustion chamber side to crankcase side. Secondly, it act as Conduction Bridge to conduct maximum quantity of heat from piston skirt side to cylinder liner side. In understudy diesel engine, 1^{st} has problem with its design. The piston group represents a complex sealing system, since three different fluids (engine oil, fuel and combustion chamber gas)

interact by means of leakage or direct mixing in the combustion chamber, as in the case of direct injection of fuel. This may result in undesirable side effects such as emission of oil into the exhaust gas, entry of fuel into engine oil or excessive emissions. The reduction of friction, while maintaining the sealing function, is therefore a trade-off point in the advancement of the piston assembly. Recently researchers are being interested to take the consideration of piston rings liner system because these are responsible to predict the wear, efficiency of engine, fuel consumption and carbon emissions in IC engines. The system includes the piston and ring pack mainly responsible for maximum friction losses which are almost 30-40 % of the whole engine assembly as shown in figure (1.1).

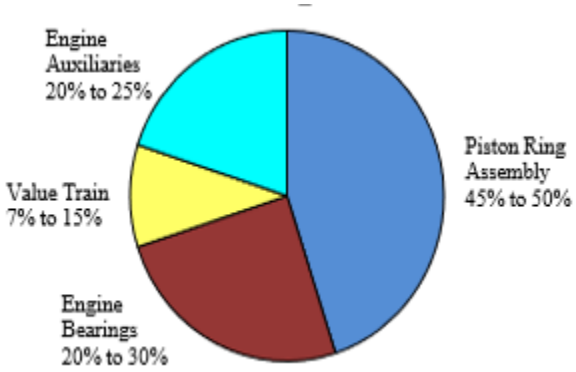

Fig 1.1 FMEP of Piston, Rings and Rods [1]

Mathematical models allow both a detailed look into the lubrication gap within ring-liner interface, along the analysis of the entire system, piston assembly with the occurring mechanical effects such as ring dynamics in the axial, radial and angular motion, ring flutter, ring collapse or the fluid flows, or their interaction. The awareness of the existence of hydrodynamic lubrication between both the rings and the liner during most of the engine operation followed, which made the optimization of the primary ring parameters. On the other hand, the flow of gas through the clearances of an engine and the flow returning to the combustion chamber have an important role, in particular, in the case of unburned hydrocarbons, on the consumption of oil and affect the efficiency and power of the engine. Piston acceleration and deceleration acts as basic force to effect the ring dynamics within the groove. On the other side, friction force again plays an important role to decide the dynamics of ring and liner interaction. For most of the time, during engine operation ring keep sitting on groove upper flank or lower groove flank. Ring and liner interaction and ring and groove surface interface are strongly interlinked which define the geometric relation of groove upper and lower flanks, ring running surface and liner interaction and ring twist.

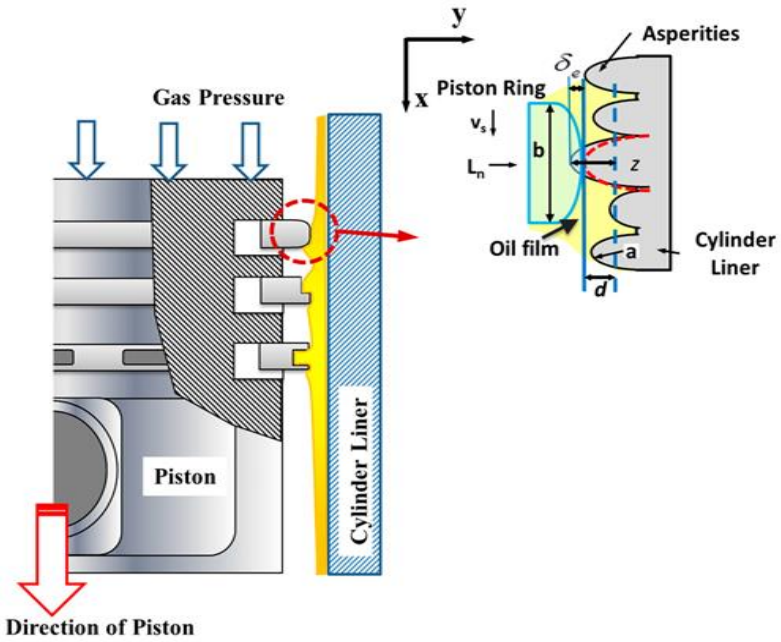

Figure 1.2 Piston Ring Pack Assembly [3]

1.3 Literature Review

[4, 5] Piston assembly working performance is effected by piston secondary dynamics and piston skirt lubrication. That is why serious focused has been put on to lubrication of piston skirt-liner interface. [6] incorporated the inertial impact of film thickness to Reynolds model; the effect of hydrodynamic friction force, oil film inertia on film pressure and lateral motions were investigated. Performed an analysis to incorporate the effect of oil film inertia in lubrication model. Hydrodynamic friction force, hydrodynamic pressure force and lateral motions were estimated. [7] Considered in the analysis instantaneous interaction of piston skirt with cylinder wall including piston secondary motion effects. [8] Proposed a model to analyze the effect of cylinder vibration on piston secondary motion and tribological behaviors of piston. [9] Developed a model to investigate the skirt temperature effect and lubrication phenomena of piston and liner wall. [10] Performed a numerical base analysis on piston secondary motions to understand the piston different designs changes on piston dynamical behavior within piston and liner wall. 11] Performed a detail study to model piston secondary motion and piston skirt lubrication phenomena including surface roughness effects.[12] Included connecting rod dynamics for the purpose to understand the piston lateral motions and cylinder liner lubrication. It was noticed that location of center of mass (COM) is crucial for connecting rod design. [13, 14] Analyzed the effect of connecting rod motion on piston secondary motion. It was noticed that effect of connecting rod motion, oil film thickness and hydrodynamic friction force cannot be ignored. [15] Performed an analysis to estimate piston secondary motions and piston-cylinder liner system. Analysis was more realistic with the inclusion of elastic and thermal deformation of both piston skirt and cylinder liner surfaces. Top ring in nomenclature is famous as first compression ring which bears mechanical and thermal loadings. Main purpose of compression ring is to provide sealing blow-by gases which trail down to crankcase side. In [16] analysis These rings have mostly parabolic and barrel type face section and having wear resistant surface coating of molybdenum Under severe wear conditions these rings have tendency to self-adjustment in the groove. In [17] study

during reciprocating motion of piston, these ring causes wear phenomenon inside the groove. Second compression ring assist upper most ring to reduce the upside lubricant oil flow, therefore, compression rings with tapered face profile or non-asymmetrical face profile don't need coated surface. Purpose of oil control rings is to improve oil transport phenomenon. [18, 19] Found that oil ring is coated with chromium plated have two running lands or faces Rings have five main factors which contributes to improve given five factors; minimum friction, good sealing capability, low emission, controlled oil flow to engine, long-life and cost effective, good bearing to thermal and mechanical loadings. [20] Performed analysis on ring lubrication incorporating elastohydrodynamic lubrication and distorted cylinder bore. Numerical based analysis proved very helpful to understand piston rings performance .Two type of analysis are being performed in recent studies static and dynamics analysis. In [21] static analysis static interaction of piston ring with cylinder is considered while in dynamic analysis consists of ring pack dynamics, piston secondary motion and blow-by effects.[22] Developed a model to measure hydrodynamic pressure between piston and liner surface interaction in heavy duty diesel engines using gauges. It was observed that phenomenon was hydrodynamics during engine cycle with different running conditions of loads, temperatures and clearances.

[23] For the first time, Reynolds proved analytically that a viscous fluid can produce enough hydrodynamic pressure to separate two physical surfaces resulted in low hydrodynamic friction and no wear. [24] Performed numerical and experimental based analysis to determine the lubricant film thickness. Calculated film thickness was enough greater and found a difference between calculated and theoretical values. Reason of this disagreement was highlighted between theoretical and experimental values. [25] Compared theoretical results with experimental results with the assumptions that both ring and liner have smooth surfaces which show surfaces conformability. It was observed that a realistic model is required to correlate the result of theoretical data with experimental data. [26] Included cavitation phenomenon in their proposed hydrodynamics regime.in their study, 2D analysis of ring including elliptical shaped distorted cylinder bore was utilized to measure circumferential flow. It was observed that hydrodynamics pressure decreases suddenly with an increase in lubricant oil film thickness due to distorted cylinder bore. A similar result has been found by [27] that when ring in second groove transits many times within the groove during the cycle, oil consumption decreases and the flow is below the piston and the oil returns to the crankcase driven by blow-by gas. It is natural to think that the consumption of oil is minimized if the second groove is removed. [29]

Developed a 2-dimensional model to measure oil film thickness in sliding direction in case of diesel engine. In the presence of squeeze effect near at TDC and BDC film thickness was predicted to be of few micron which indicates that wear rate may enhanced in a region near at TDC and BDC. When moving the piston along the liner and tilting it generating the cylinder to the opposite side. [30] Developed a model to study the ring motions in radial axial and angular direction including the ring end variable gap. [31] Observed that twist of piston ring greatly affect the lubrication between ring and liner interface. It was also noticed that there may be a possible flutter of ring occurs at outer area of groove. This analysis was performed without taking effect of gas flow under the assumption of quasi steady state analysis. [32] Took ring as beam element and model it by FEM method besides radial, axial and twist motions were studied. [4, 12, 13] Developed a model to define the ring dynamics as well as gas flow. They took the analysis to determine the gas flows between ring and groove interface, but they did not include the twist angle. Measurements showed that gas flow have influence on ring motion. A study have been conducted on ring axial motion within the groove which includes individual model for ring axial motion and

lubrication model. It was shown that friction force has very small effect in comparison to other ring surface forces. A more realistic insight was developed by [36, 37] to optimize piston ring pack In another study, a theoretical model was developed for complete ring pack analysis which includes 2-D asymmetric detailed analysis with the emphasis on the interaction between supermodels between ring and liner interaction and ring and groove interaction [38] was performed on ring interaction between groove and liner to understand ring dynamics and oil consumption mechanism. [39] Developed a model was developed to consider the non-asymmetric analysis by taking the oil flow along the circumference of liner [40] Performed a detailed study to take 3-dimensional analysis for ring liner lubrication. [41] Took cylinder distorted shapes of bore such as parabolic elliptical and four lobes of distorted bore were taken into account including oil damping effect near TDC and BDC of a stroke. It was observed that effect of distorted bore causes minimum energy consumption excluding effect of ring liner interaction. [42] Considered effect of elastorhydrodynamic lubrication (EHL) regime in ring-liner lubrication with inclusion of film squeeze effect.

In this research work, understudy high torque low speed diesel engine has faulty ring design. This faulty design of ring causes the lubricant oil to mix with fuel in combustion chamber which burns due to which lubricant oil consumed. Oil consumption results in insufficient lubrication which promotes wear of first compression ring. This wear phenomenon reduce engine life cycle.

1.4 Methodology

First for piston secondary motion, initial values of top and bottom eccentricities 'e_t' and 'e_b'are initialized. At time zero, initial values of top and bottom eccentricities are assumed zero for first crank angle calculation. After each iteration, piston dynamic balance is checked. Once, piston dynamic balance is satisfied then respective velocities and accelerations in lateral direction are calculated. Then next iterations for next crank angle are performed. Ring hydrodynamic pressure will be solved numerically based on initially assumed by discretizing Reynolds equation then Reynolds equation is solved iteratively by successive over relaxation method (SOR). Once the radial balance is satisfied then minimum oil film thickness will be updated for next crank angle. Ring axial motion within groove will be solved by RK-4 method. Initially, ring is considered at groove upper flank. At time = 0, ring axial position is taken equal to zero. When the ring axial balance of forces is satisfied then ring axial position is updated for the next crank angle.

CHAPTER 2

PISTON SECONDARY MOTION

In engine tribology piston assembly have been recognized an important part to understand the tribological behaviors. Piston acts as sliding bearing and shows reciprocating motion which is called primary motion. Piston also shows two other motions in lateral direction which is due to clearance in radial direction perpendicular to cylinder surface and other is due to piston tilt in angular direction, this tilt motion is basically generated based on top and bottom eccentricity. Piston is actually is a long slider bearing and have mostly parabolic profile that is the reason it has two different piston top clearance and bottom side clearance. Piston lateral and tilt movements are results of imbalance of forces acting on piston surface during piston motion between TDC and BDC. In piston assembly major factor which involve measuring the performance of assembly parts such as friction losses, wear measurement, power losses are highly based on dynamics and lubrication. Radial clearance is also main contributor in all these losses due to small clearance in radial direction is a big cause of friction losses which ultimately enhance the power losses.

2.1 Model Formulation

Piston in the cylinder shows axial motion while crank shaft shows rotational motion due to piston. Piston assembly is shown in the figure (2.1). Combustion gas force is directly applied on the piston crown area. Piston inertial force and wrist piston pin inertial force which are $\overline{F_{IP}}$ and $\overline{F_{IC}}$ are produced by piston motion in the cylinder and moments due to piston secondary motion are M_{IC} , M_h , M_f . Friction force and friction moments are M_{fh} and F_{fh} respectively. Connecting rod force and moments are respectively F_{cr} and M_{cr}.

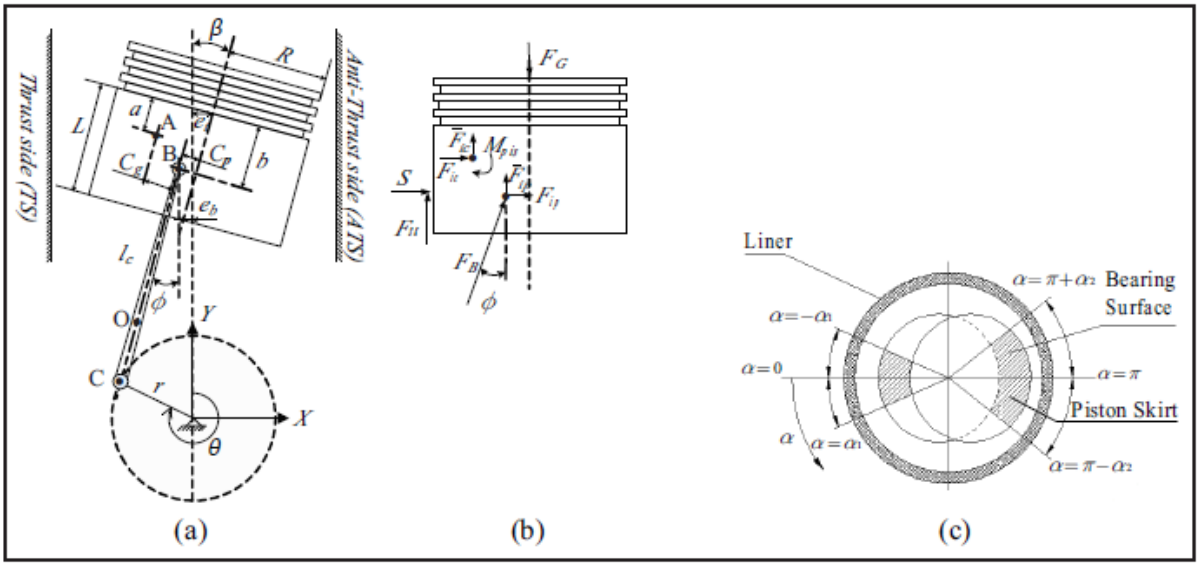

Figure 2.1 Forces Acting on Piston and Tilt Motion [6]

Piston axial position, velocity and acceleration are function of crank angle and can be written as,

$$Y = (\,(\,L + r\,)^2 - {C_p}^2\,)^{0.5} - (\,L^2 - B^2\,)^{0.5} - r * \cos\Psi \qquad (2.1)$$

Piston speed can be written as,

$$V = \dot{Y} = r\omega \sin\Psi + r\omega B\cos\Psi\,[-B^2\,]^{0.5} \qquad (2.2)$$

Piston primary acceleration is given by,

$$\ddot{Y} = r\omega^2 \cos\Psi + (r\omega B\cos\Psi)^2 (L^2 - B^2\,)^{-1.5} + [\,(r\omega B\cos\Psi)^2 - r\omega^2 B\sin\Psi\,](L^2 - B^2\,)^{-1.5} \qquad (2.3)$$

Where,

$$B = C_p + r\sin\Psi \qquad (2.4)$$

Piston inertial force and wrist pin inertial force in reciprocating direction are given as,

$$\overline{F_{IP}} = -m_{pin}\ddot{Y} \qquad (2.5)$$

$$\overline{F_{IC}} = -m_{pis}\ddot{Y} \qquad (2.6)$$

Connecting rod changes its angle during engine operation which is given by,

$$\phi = \operatorname{atan}[B * (L^2 - B^2\,)^{-0.5}] \qquad (2.7)$$

Piston lateral force and moment depends on top and bottom eccentricities given as,

$$F_{IP} = -m_{pin} * \left[\ddot{e}_t + \frac{a}{L}(\ddot{e}_b - \ddot{e}_t\,)\right] \qquad (2.8)$$

$$F_{IC} = -m_{pis} * \left[\ddot{e}_t + \frac{b}{L}(\ddot{e}_b - \ddot{e}_t\,)\right] \qquad (2.9)$$

$$M_{IC} = -I_{pis}\frac{(\ddot{e}_b - \ddot{e}_t\,)}{L} \qquad (2.10)$$

Equilibrium of all forces is given by,

$$F_G + F_{fh} + \overline{F_{IP}} + \overline{F_{IC}} + \overline{F}\cos\Psi = 0 \qquad (2.11)$$

$$F_h + F_{IP} + F_{IC} + \overline{F}\sin\Psi = 0 \qquad (2.12)$$

$$M_h + F_{IC}(a - b) + M_{IC} - \overline{F_{IC}}C_g + F_G C_P + M_f = 0 \qquad (2.13)$$

Piston angular motion in the cylinder is between major thrust side and minor thrust side are given. In radial direction piston have clearances on the top and bottom side given as e^t and e^b respectively. In figure (2.1) shown piston circumferential motion as piston and piston pin inertial force due to piston secondary motion are given as a system of equilibrium equation for piston, piston pin and connecting rod can be written in matrix form given as,

$$\begin{bmatrix} m_{pin}\left(1-\frac{a}{L}\right)+m_{pis}\left(1-\frac{b}{L}\right) & m_{pis}\left(\frac{a}{L}\right)+m_{pis}\left(\frac{b}{L}\right) \\ \left(\frac{I_{pis}}{L}\right)+m_{pis}\left((a-b)\left(1-\frac{b}{L}\right)\right) & m_{pis}\left((a-b)\frac{b}{L}\right)-\left(\frac{I_{pis}}{L}\right) \end{bmatrix} \begin{pmatrix} \ddot{e}_t \\ \ddot{e}_b \end{pmatrix} = \begin{bmatrix} F_h+F_s+F_{fh}\tan\phi \\ M_h+M_s+M_f \end{bmatrix} \quad (2.14)$$

Bore diameter	150
Stroke length	0.3888
Connecting rod length	141
Speed	2000 RPM
Ring axial clearance hL	2e-5
Ring axial height	2.46e-3
Ring width	5.34e-3
Ring mass	0.022
Wrist pin offset cp	1.04e-4
Geometric parameter of ring face profile s2	2e-6
Crank radius	0.1944 m
Error	0.001
Ring groove clearance	5e-6
First land temperature	600+273

Table 5.1 Parameters

2.2 Piston Skirt Lubrication

Forces acting on skirt from different models required to define piston motion. Most crucial sub model is piston hydrodynamic lubrication. This model contains 2-dimensional case for Reynolds lubrication model is utilized to determine the hydrodynamic pressure based on initially assumed oil film thickness which act as primary hydrodynamic force on piton skirt at every crank angle. An average 2 D Reynolds equation incorporates the effects of friction losses, power losses and wear rate.

2.2.1 Oil Film Thickness

Lubricant oil film thickness between two parallel plates is an important parameter which is needed to calculate hydrodynamic pressure given by the equation as,

$$\overline{h} = C + e_t\cos x + [\ e_b - e_t\ ]\frac{y}{L}\cos x \qquad (2.15)$$

2.2.2 Non-dimensional Form of Lubricant Film Thickness

This non-dimensional form of lubricant oil film thickness is differentiated w.r.t x and y, because this parameter is needed by computational scheme used in Reynolds equation. Expressions of derivatives of oil film thickness are given below,

$$\overline{h^*} = 1 + E(t)_t \cos x^* + [\ E(t)_b - E(t)_t\ ] y^* \cos x^* \qquad (2.16)$$

2.2.3 Hydrodynamic Pressure

Hydrodynamic pressure in case of piston skirt lubrication can be measured by 2-dimensional Reynolds equation. Reynolds equation in dimensional form can be written as,

$$\frac{\partial}{\partial x}\left(\frac{h^3}{12}\frac{\partial p}{\partial x}\right) + \frac{\partial}{\partial y}\left(\frac{h^3}{12}\frac{\partial p}{\partial y}\right) = 6\left(U\mu\frac{dh}{dx}\right) \qquad (2.17)$$

2.2.4 Vogelpohl Parameter

Dimensionless form of Vogelpohl parameter can be written as,

$$M_v = p^* {h^*}^{1.5}$$

$$\frac{\partial}{\partial x^*}\left(\frac{{h^*}^3}{12}\frac{\partial p^*}{\partial x^*}\right) + \left(\frac{R}{L}\right)^2 \frac{\partial}{\partial y^*}\left(\frac{{h^*}^3}{12}\frac{\partial p^*}{\partial y^*}\right) = \frac{\partial h^*}{\partial x^*} \qquad (2.18)$$

$$\frac{\partial^2 M_v}{\partial {x^*}^2} + \left(\frac{R}{L}\right)^2 \frac{\partial^2 M_v}{\partial {y^*}^2} = F M_v + G \qquad (2.19)$$

$$F = \frac{0.75 * [\ \left(\frac{\partial h^*}{\partial x^*}\right)^2 + \left(\frac{R}{L}\right)^2 \left(\frac{\partial h^*}{\partial x^*}\right)^2\ ]}{{h^*}^2} + \frac{1.5 * [\frac{\partial^2 h^*}{\partial {x^*}^2} + \left(\frac{R}{L}\right)^2 \frac{\partial^2 h^*}{\partial {y^*}^2}\ ]}{h^*} \qquad (2.20)$$

$$G = \frac{\left(\frac{\partial h^*}{\partial x^*}\right)}{{h^*}^{1.5}} \qquad (2.21)$$

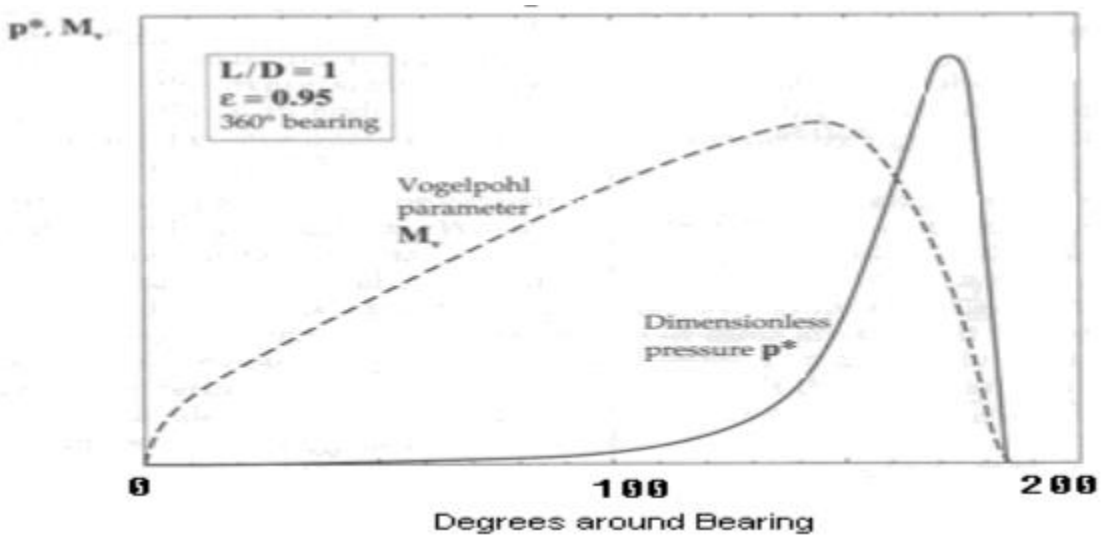

Figure 2.2 Variation of dimensionless pressure and Vogelpohl parameter along the center plane of a hydrodynamic bearing [20]

2.2.5 Hydrodynamic Force

Hydrodynamic pressure distribution on ring surface is needed, which may be calculated by Reynolds equation for 2-dimensional parallel surfaces. This hydrodynamic pressure is integrated on the whole ring surface area to calculate hydrodynamic force normal to surface.

$$F_h = R \iint p_h(\theta, y)\cos\theta d\theta dy \qquad (2.22)$$

2.2.6 Hydrodynamic Moment

When hydrodynamic force is measured, then moment of this force about wrist pin can be find by the given equation.

$$M_h = R \iint p_h(\theta, y)(a - y)\cos\theta d\theta dy \qquad (2.23)$$

2.2.7 Hydrodynamic Friction Force

Friction force due to internal friction within lubricant layers can be determined by the given equation. First of all shear rate in term of viscosity is find then shear rate is integrated to calculate Hydrodynamic friction force,

$$F_{fh} = R \iint \tau(\theta, y)\cos\theta d\theta dy \qquad (2.24)$$

Average shear stress can be written as,

$$\tau = \eta \frac{U}{h} + \frac{h}{2}\frac{dp}{dy}$$

Implement this $'\tau'$ in equation (2.24)

$$F_{fh} = R \iint (\eta \frac{U}{h} + \frac{h}{2}\frac{dp}{dy}) d\theta dy \qquad (2.26)$$

Shear stress 'τ' is integrated on the whole cylinder region to measure hydrodynamic friction force with in lubricant oil film thickness. The coefficient of hydrodynamic friction is evaluated by the ratio which is performed between the non-dimensional friction force is divided by non-dimensional hydrodynamic load. Thus, for piston case hydrodynamic friction coefficient is the division between the friction force and hydrodynamic pressure force,

$$\mu = \frac{\text{Friction force}}{\text{Load}} = \frac{\iint \tau \, dxdy}{\iint p \, dxdy}$$

2.2.8 Hydrodynamic Friction Force Moment

Friction force within lubricant oil film acts parallel to the whole cylinder surface which produces moment about wrist pin is given by,

$$M_{fh} = R \iint (\eta \frac{U}{h} + \frac{h}{2}\frac{dp}{dy})(r\cos\theta - C_p)d\theta dy \qquad (2.27)$$

2.3 Numerical Solution Procedure

Hydrodynamic force in initially unknown which is calculated by integrating hydrodynamic pressure on the skirt surface. In order to solve combined hydrodynamic pressure and piston secondary motion, first it is needed to determine the forces acting on the skirt surface as a function of transverse motions and their first-time rates. It is assumed that these transverse movements are initially known at crank angle, solve the complete piston dynamics. Numerical convergence and stability are much complex by explicit numerical methods. Presently, we characterize the conditions on boundary and extend of values to be measured after setting up the controlling relation. It is noticed that boundary nodes of piston ring region exist at a predefined value equal to zero, on the other hand, for all other nodes numerical solution is measured by finite difference method (FDM). The space in both the cases (piston rings) is the total slider bearing with limits of 'y*' from -0.5 to +0.5 and the central boundary vanishes.

1. Assumed initial time step, time step is linked with crank angle so 'h' oil film thickness can be measured instantaneously with respect to time and crank angle. Then hydrodynamic force is measured by integrating the lubricant hydrodynamic pressure within the oil film thickness.
2. For piston dynamics, initial values of top eccentricity 'e_t' and bottom eccentricity 'e_b'are initialized. For the current time step, velocities $\dot{e}_t$ and $\dot{e}_b$ are calculated. Similarly based on these velocities' current values of acceleration $\dot{e}_t$ and $\dot{e}_b$ are calculated.
3. Then we check weather piston main dynamics model is satisfied or not for current values of acceleration. If it is satisfies we, iterate it for next time step by given relations,

$$e_t\,(t_i + \Delta t) = e_t(t_i) + \Delta t\, \dot{e}_t(t_i)$$
$$e_b\,(t_i + \Delta t) = e_b(t_i) + \Delta t\, \dot{e}_b(t_i)$$

4. Initial guess for $e_t = 0$, $e_b = 0$, $e_t dot = 0$ $e_b dot = 0$ given as,
$$e_t = 0,\ e_b = 0,\ e_t dot = 0\ e_b dot = 0$$
5. It piston dynamics model is not satisfied we update the initial value for e_t and e_b and again solve it numerically by Rk-4 method. This is repeated until we get converged solution.
6. Once the solution is converged, the solution can be obtained at any possible piston position.
7. A converged solution meet the given below criteria,

$$e_t(t) = e_t(t + \frac{4\pi}{w})$$
$$e_b(t) = e_b(t + \frac{4\pi}{w})$$
$$\dot{e}_t(t) = \dot{e}_t(t + \frac{4\pi}{w})$$
$$\dot{e}_b(t) = \dot{e}_b(t + \frac{4\pi}{w})$$

Main equation of piston dynamics model is numerically solved by Rk-4 method. Simulations run for real time in one complete engine cycle. Crank angle vary from 0 deg. to 720 deg. Time is linked with crank angle with rpm by the given relation,

$$\theta = wt$$

CHAPTER 3

MATHEMATICAL MODEL of GAS FLOW

Ring groove crevice volumes are divided into different regions. Groove pressure can be predicted by gas flow model coupled with ring dynamics. Blow by gases are the burnt gases trail down from the combustion chamber side to crankcase side. These hot gases mixed with oil in the sump which contaminate the lubricant oil due to which oil consumption increases, as a result for proper lubrication lubricant oil is need to be replaced again and again. This blow by effect cannot be avoided due to clearances between ring groove as well as ring and liner side. Due to this blow-by phenomenon, fuel efficiency reduces and lower the engine performance. Areas normal to the changing clearances are related to ring axial motion. So the gas flow are determined based on the changing clearances. In addition, gas flow also decided based on the ring end gap which provide the direct path to blow-by gases from upper land to the lower consecutive land. Main role of ring is to proper sealing to meet all requirements including ring dynamics. Gas mass flow rate varies within ring groove clearance. These land clearances and groove clearances are interconnected by different flow paths. Those grooves volumes has been divided by lands and regions are shown in figure (3.1). This diagram demonstrates the clear picture of piston skirt along with ring pack. Ring pack includes normally three different rings the upper most ring placed in the first groove is known as 1st compression ring. Ring placed in the second ring is known as oil control ring and the ring placed in the third groove is known as oil scraper ring. Region 1 is defined by top land just below the combustion chamber region. This land is divided by plane a which separate top land from combustion chamber and plane b is located just at the start of region 2. Pressure drop through region 1 is negligible therefore pressure on plane 2 is assumed equal to pressure in combustion chamber. Further, consideration was given and it is taken uniform pressure in other regions within groove. As clearances keep changing during engine operation so gas flow is determined by orifice flow models. Clearances within rings and their respective grooves and ring end gaps decide the gas leakage from combustion to crank case side. Crevice regions are given numbering 1 to 5 .Each ring is interconnected by two consecutive regions connected by the ring end gap. Based on the ring present location regions within the groove are connected by clearances between ring grooves with region 1. During compression stroke, ring initially sit on the lower groove flank region 1 and region 2 are directly interconnected. When direction of forces changes during expansion stroke first ring start moving to the other side of the groove to the upper groove region 2 and region 3 come in direct connection. Upside clearance decreases due to which groove upper flank seals with ring upper surface. In this way, ring block the flow path between groove upper side to ring upper surface. Ring position in axial direction only time dependent but it is strongly coupled with gas flow model defined ring axial location in term of crank angle.

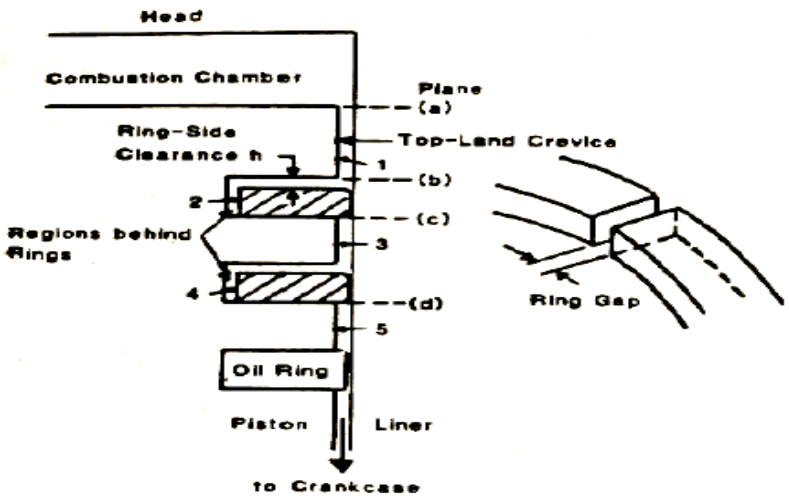

Figure 3.1 Gas Blow-by diagram [33]

It is shown in the figure (3.1) that regions are interconnected with different ring crevice volumes. Top land is directly connected with combustion chamber. Depending on ring position in groove the regions are connected with clearances.

3.1 Gas Flow Model

Gas flows occurred between different clearances interconnected by series of channels exist within ring and groove spaces. This flow is considered an isentropic gas flow because the temperature of the groove is taken as constant value. The gas flow rates are not constant due to abrupt fluctuation of pressure within groove. The main causes of these gas flows are liner bore distortions and ring end gap. Ring axial motion is also another great contributor of different gas flows because ring axial position changes due to surface forces acting on the ring.
Some important assumption are taken to analyses the gas mass flow rates through different regions divided between combustion chambers side and crank case side.
These assumptions are:
1. Pressure inside a groove remains constant. Pressure in the top land is equal to pressure in combustion region. Similarly, in the lower land there assumed crank case pressure.
2. Iso-thermal flow of gas is assumed in the groove. It is considered temperature on the piston wall is same to the liner wall.
3. Chemical properties of gas remains constant in different crevice volumes.
4. Shape of cylinder bore is not circular. Cylinder bore is taken of elliptical shaped. Two lobes are taken around the cylinder bore circumference.
According to law of conservation of mass pressures in respective groove can be found by the given equation,

$$P_1 = \text{combustion gas pressure}$$

$$\frac{m_{02}}{P_{02}}\frac{dP_2}{dt} = \dot{m}_{12} - \dot{m}_{23} \qquad (3.1)$$

$$\frac{m_{o3}}{P_{o3}}\frac{dP_3}{dt} = \dot{m_{13}} + \dot{m_{23}} - \dot{m_{34}} - \dot{m_{35}} \qquad (3.2)$$

$$\frac{m_{o4}}{P_{o4}}\frac{dP_4}{dt} = \dot{m_{34}} - \dot{m_{45}} \quad (3.3)$$

$$P_5 = \text{crank case pressure}$$

P_1 is combustion pressure it has been measured by experimentally as shown in figure (3.1). Here i = 1,.., 4 for Pi show pressure in different crevice volumes. Similarly, P_{o2}, P_{o3} and P_{o4} represents the initial pressures respectively in regions 2, 3, 4. On the same side m_{02} , m_{03}, m_{04} gives masses in respective regions for i = 2,…,4. For i = 1,..,4 , where $\dot{m_{ij}}$ are the different mass flow rates in respective crevice volumes for P_{o1}, P_{o2}, P_{o3}, P_{o4} and temperature on cylinder wall.

$$\dot{m_a} = \frac{m_{01}}{P_{o1}}\frac{dP_1}{dt} + \dot{m_b}$$

$$\dot{m_b} = \dot{m_{13}} + \dot{m_{12}}$$

$$\dot{m_c} = \dot{m_{13}} + \dot{m_{23}}$$

$$\dot{m_d} = \dot{m_{35}} + \dot{m_{45}}$$

Here, P_1 represents the pressure in combustion chamber. Mass flow rates for planes a-d are given as $\dot{m_a}$, $\dot{m_b}$, $\dot{m_c}$, $\dot{m_d}$.

One of the above equation can be solved long with above equations to calculate the unknown pressure in different crevice regions and gas flow rate through regions connected with clearances. To determined mass flow rate through land 1 is more interested because it is helpful to estimate the timing of flow of gas through different regions. There comes an instant when pressure which acts on the back of the ring gets similar value to the pressure in combustion side flow change its direction in opposite to the coming flow. Flow timing of top land is controlled by crevice volume connected by regions which changes with change in clearance.

3.2 Mass Flow Rate of Gas through Groove Clearance

Mass flow rate of gas can be determined by considering compressible and iso-thermal between ring and groove side clearance. Clearance channel between ring and groove height 'h' and width 'Wr'. Iso-thermal flow is considered because gas slow rate of gas flow maintain at constant temperature during engine operation [33]. Mathematically gas flow between the clearance change within ring and groove can be determined as ,

$$\left(\frac{\dot{m}}{A}\right)^2 = \frac{{P_u}^2 - {P_d}^2}{RT\left(\frac{4fW_r}{D} + 2\ln\left(\frac{P_u}{P_d}\right)\right)} \qquad (3.5)$$

Where D is hydraulic diameter which is $D = 2h$. As gas flow is taken laminar within clearance , so f= 4/Re and Re= $\left(\frac{\dot{m}}{A}\right)\frac{D}{\mu_{gas}}$ .Most of the time , it is $2\ln\left(\frac{P_u}{P_d}\right) << \left(\frac{4fW_r}{D}\right)$.Above equation (3.5) can be written as,

$$\left(\frac{\dot{m}}{A}\right)^2 = \frac{h^2({P_u}^2 - {P_d}^2)}{24\mu_{gas}W_r RT} \qquad (3.6)$$

Where diameter of hydraulic is D = 2h.

A= Area in normal direction to the flow

F = coefficient of friction
T = Temperature on ring surface
R= Gas constant

3.3 Groove Pressure Equation

Given model is utilized in the present study developed by [33] study to find the gas flow between ring and groove. In this work, just first compression ring is focused to find gas flow between ring and groove clearance. Similar model is used to find the gas flow rates through others regions linked by lands.
Here, only first compression ring is under focused so the study in limited to the first compression ring and groove. According to assumptions, pressure in groove remains constant .So groove pressure at any time instant can be evaluated by the given relation,

$$\frac{V_2}{pi*BRT}\frac{dP2}{dt} = \frac{{h_{12}}^3({P_1}^2-{P_2}^2)}{24\mu_{gas}W_rRT} - \frac{{h_{23}}^3({P_2}^2-{P_3}^2)}{24\mu_{gas}W_rRT} \qquad (3.7)$$

Similarly, gas flow model to measure actual cost of lubrication of oil

CHAPTER 4

RING DYNAMICS

4.1 Ring Dynamics

Forces and moments acting on ring surface are responsible for ring dynamics defined as axial motion, radial motion and twist motion within the groove. These forces and moments includes tension force, inertial force, hydrodynamic force between ring and liner, hydrodynamic friction force and friction force due to rough surfaces.
The radial clearance is essential to allow the ring to show free motion. If the gas pressure force at the backside of the ring is too weak, the radial movement of the ring is minute.

4.1.1 Axial Motion

The movement in the groove must be sufficient so that, under the effect of the high temperatures to which the ring groove is subjected, its ends do not come into contact. This can result in either a rupture of the ring or its exfoliation. On the other hand, a movement with excessive clearance reduces the tightness of the gas and causes an increase in blow-by gas. We will see in the chapters following, the influence of motion within groove on the sealing of gas blow-by.
In axial direction, groove reaction Rx between ring and groove flanks can be described easily based on ring position within groove. The ring start its motion as the total sum of forces changes the direction. As long as the summation of forces remains zero the ring keeps seating on the upside or lower side of groove flank. When the combined effect of forces change force the ring o move to the opposite side of the groove. This is defined by the ring equation of motion in axial direction. Ring completes its motion is defined by the center of gravity of ring cross section. Ring axial motion depends on the relative lift between ring surfaces and groove flanks. Too little axial movement prevents the ring to move in its groove from where, risk of pinching then of a scrubbing of the groove. Too much axial movement favors oil lifts, located at the bottom of the groove, towards the combustion chamber and causes the grooves and excessive consumption of oil by the engine.
Here, Ring motion within groove in axial direction will be considered. Ring and groove surfaces are assumed smooth. There exist enough work on ring axial motion within the groove. Change in ring lift between upper and lower surfaces of groove determined the ring position within groove.

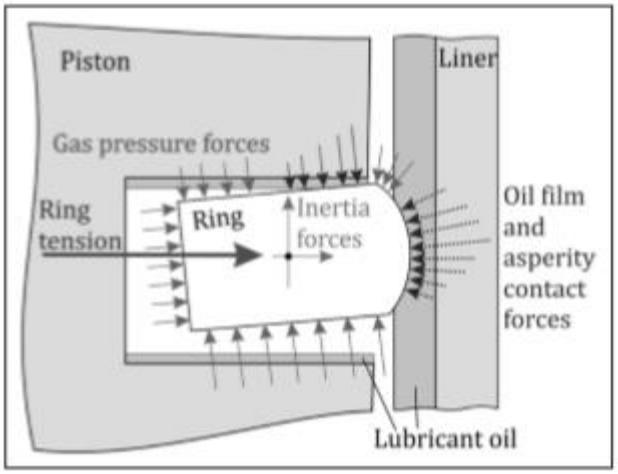

Figure 4.1 Forces and Moments Acting on Ring Schematic diagram [2]

4.1.2 Hydrodynamic Friction Force

Hydrodynamic friction force due to internal friction within oil film thickness can be evaluated by integrating the shear rate on the whole surface area which is given by,

$$F_{vis} = \int_0^L \int_0^b \tau \, dxdy \qquad (4.1)$$

where

$$\tau = \eta \frac{U}{h} - \frac{h}{2} \frac{dp}{dy}$$

$$F_{vis} = \int_0^L \int_0^b \eta \frac{U}{h} - \frac{h}{2} \frac{dp}{dy} \quad dxdy \qquad (4.2)$$

4.1.3 Upper Gas Pressure Force

Upper gas pressure force which acts on the ring upper surface can be estimated given as,

$$F_{gas,Upper} = \left(\frac{P_1 - P_2}{2}\right) \qquad (4.3)$$

4.1.4 Lower Gas Pressure Force

Lower gas pressure force acts on the bottom ring surface can be written as,

$$F_{gas,Lower} = \left(\frac{P_2 - P_3}{2}\right) \qquad (4.4)$$

4.1.5 Ring Tension Force

When the ring is properly position within the cylinder results in ring elastic deflection due to the ring flexibility. Ring tension force is shown below.

$$F_{tention} = (P_{tention} A)$$

$$P_{tention} = \left(\frac{\sigma_{bending,stress} \quad b^2}{3D(D-b)}\right) \qquad (4.5)$$

Where b = Ring width, D = diameter of ring.

Contact pressure is determined based on the ring material characteristics such as modulus of elasticity as well as ring geometric relation. In fact, the experimental based calculation of tension force is complicated and so for the purpose it may be determine in term of tangential force acting at the ends of the ring.

$$\sigma_{bending,stress} = \left(\frac{3\,Eb\,f}{2\,L^2}\right) \qquad (4.6)$$

Where f = Ring end gap, L = Length of ring, E = Elastic modulus of ring.

4.1.6 Inertial Force

F_i is the external force due to piston inertial effect which is needed to move the ring with piston motion and is always opposite to the direction of piston acceleration 'ap' . In case, when ring is sitting on the groove same opposite inertial force '$-m_r a_p$' is required to move ring with piston acceleration.Inertial force because of ring mass is given as,

$$F_i = m_r a_p$$

$$m_r = \text{Mass of ring}$$

$$a_p = \text{Acceleration of piston}$$

$$F_i = \text{Inertial force}$$

Ring motion in axial direction becomes,

$$m_r \frac{d^2 h_L}{dt^2} = F_{Gas,Upper} + F_{Gas,Upper} + F_{vis} + F_i \qquad (4.7)$$

$$h = \text{Ring axial lift}$$

4.2 Radial Force Balance

In radial direction, forces acting on ring front surfaces and gas back pressure are balanced at every time instant. Ring radial movement can be described well by minimum film thickness which varies during ring running conditions.

$$m_r \frac{d^2 h_{film}}{dt^2} = F_h + F_g + F_t \qquad (4.8)$$

F_h = Hydrodynamic force, F_g = Gas pressure, F_t = Ring tension force

4.3 Ring Angular Motion

Angular motion of ring within groove is dependent on moments produced by ring axial and ring radial forces acting on ring surfaces. Twist of ring can be described by the equation,

$$I \frac{d^2\alpha}{dt^2} = M_h + M_g + M_{fr} + M_t \quad (4.9)$$

α = Ring angular motion within groove, M_h = Hydrodynamic moment, M_{fr} = Friction force moment, M_t = Ring Tension moment

4.4 Numerical Procedure

Pressures within the crevice volumes are coupled with axial motion as well as with radial force balance. A scheme is developed for groove pressure coupled with ring axial motion as well as incorporated ring radial force balance. RK-4 method is used to solve numerically second order non-linear equation of axial motion coupled with groove pressure equation. Initial values are updated for every time instant until the axial positions of ring and pressure comes within acceptable defined criteria. Outcomes of blow-by model are groove pressure which are used to balance the ring radial forces .In this way, at every time instant radial force balance is made conform.

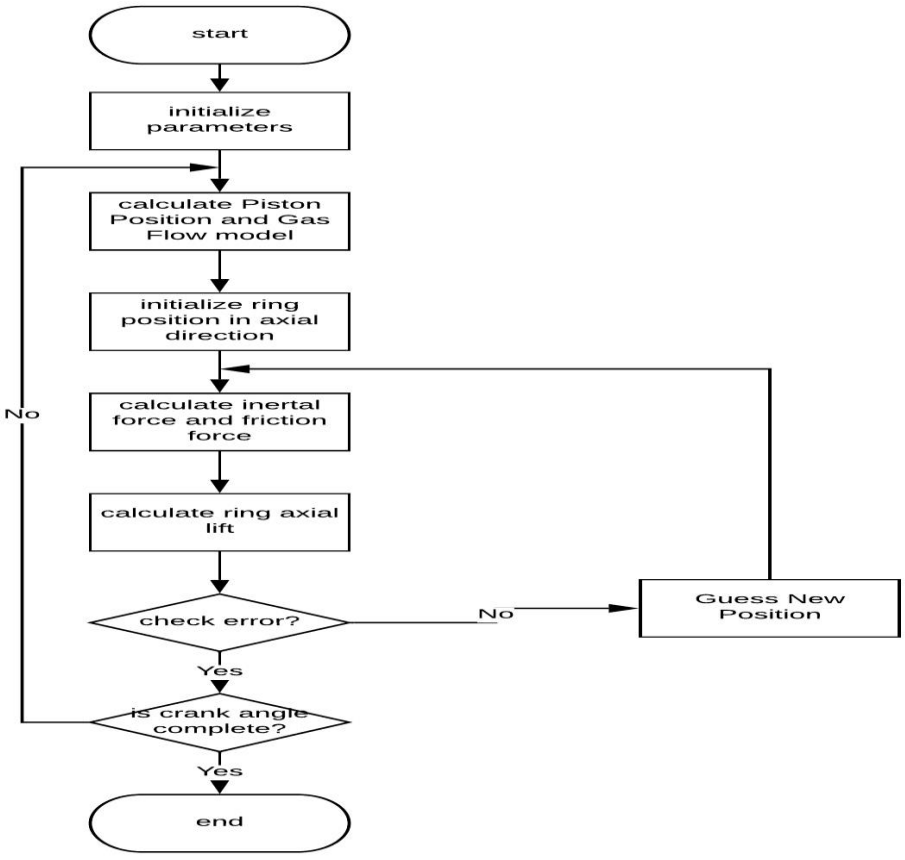

Figure 4.2 Flow Chart of Ring Axial Motion

CHAPTER 5

RING AND CYLINDER LINER LUBRICATION

5.1Mathematical Formulation of Ring Cylinder Liner Lubrication

In this chapter 2-dimensional model of hydrodynamic lubrication is given based on following assumptions given below, Laminar and incompressible flow is taken in the analysis

1. Roughness of surfaces, leakage from side surfaces and starvation of oil between plates are ignored
2. Piston is considered at static position ring position changes in radial direction
3. Viscosity is taken as constant in circumferential and sliding direction
4. Effects of piston secondary motion were not considered
5. Reynolds exist conditions and fully flooded conditions at inlet and outlet are implemented
6. It is assumed that ring-liner surfaces are smooth
7. No thermal expansion and thermal deformation were incorporated

In the present model, Reynolds equation for steady state case is taken as,

$$\frac{\partial}{\partial x}\left(\frac{h^3}{12}\frac{\partial p}{\partial \mathrm{x}}\right)+\frac{\partial}{\partial y}\left(\frac{h^3}{12}\frac{\partial p}{\partial \mathrm{y}}\right)=6\left(U\mu\frac{dh}{dx}\right) \qquad (5.1)$$

Here x shows the axial direction or sliding direction of ring, whereas, y shows circumferential direction. U Shows the piston ring velocity, h represents oil film thickness and p shows the hydrodynamic pressure. Figure (5.1) indicates the ring width, x_1 indicates the location of leading edge when ring is running toward BDC and x_2 indicates the location of trailing edge based on the ring sliding direction. These directions gets inverted when ring is moving toward BDC. q_{x2} is the flow rate in sliding direction U shows piston reciprocating velocity in axial/sliding direction, h_o indicates minimum the oil film and B is geometric parameter which shows the width of ring.

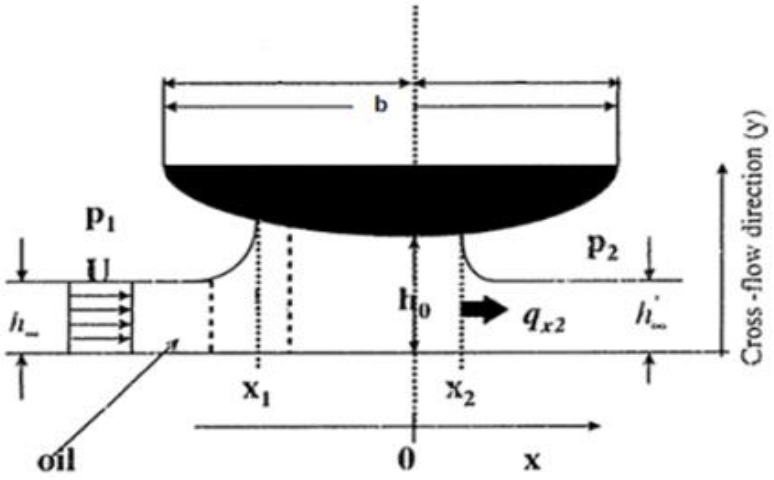

Figure 5.1 Variables and Coordinate system [36]

5.2Ring Instantaneous Velocity

According to assumption, it was assumed that ring and piston velocity is same and taken as rigid body. In sliding direction, ring have same speed as piston. In the present work, ring velocity is determined in term of crank angle. Instantaneous velocity of ring is function of crank angle θ. Piston speed at every time instant can be estimated by the given equation,

$$U=r\omega sin\theta+(Cp+rsin\theta)cos\theta(l2-(Cp+rsin\theta)2)0.5 \qquad (5.2)$$

U represents piston reciprocating velocity ,C_p represents wrist pin offset, r is used for crank radius, w shows angular velocity and L represents length of connecting rod can be represented by the given relation,

$$\omega=V/r \qquad (5.3)$$

ω = indicates engine speed rpm

5.3 Lubricant Film Thickness

In the present analysis, lubricant oil film thickness was considered both in axial (sliding) direction as well as in circumferential direction along the cylinder. This model includes the ring running profile and distorted cylinder bore effect. Oil film equation in circumferential and sliding direction is defined by the given relation,

$$h(x,y) = h_1(x) + h_2(y) + h_0 \qquad (5.4)$$

Film thickness in case of hydrodynamics lubrication is find by the given above equation. $h_1(x)$ is film thickness in sliding direction similarly $h_2(y)$ is film thickness along the circumferential direction around the ring. h_0 Shows the nominal minimum film thickness initially set to meet a specific convergence criteria. If a set criteria successfully meet then next value of film thickness is updated. In case of only rigid hydrodynamic lubrication all three $h_1(x), h_2(y)$ and ho have same value.

5.4 Oil Film Thickness in Sliding Direction

Minimum film thickness can be predicted based on the ring front face shape. Ring face profile for barrel shape ring in ring sliding direction is divided into three piecewise. Mathematical relation of these functions can be written as,

$$\begin{cases} S_1(x^2 - 2a_1x + {a_1}^2) & -b/2 \le x \le a_1 \\ 0 & a_1 < x < a_2 \\ S_1(x^2 - 2a_1x + {a_1}^2) & a_2 \le x \le b/2 \end{cases} \qquad (5.5)$$

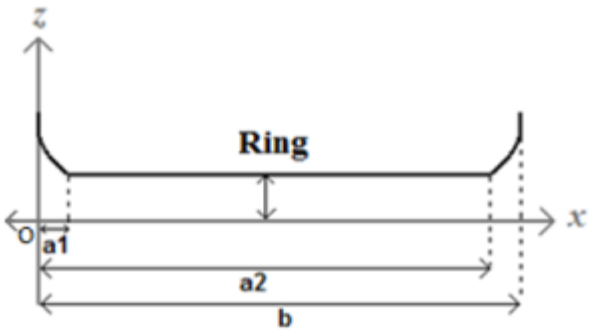

Figure 5.2 Ring Face Profile [20]

Ring face profile is defined by geometric parameters a_1, a_2, S_1, S_2 .Change in these parameters change the geometry of ring, consequently, change the tribological behaviors such as friction losses, wear, power losses and flow rate. In this case symmetric ring was utilized which have equal a1 and a2. Whereas, for asymmetric ring a_1 and a_2 are different.

5.5 Circumferential Lubricant Film Thickness

Numerous researches have included effects of perfect cylinder bore in analysis of hydrodynamic lubrication. For real analysis this effect is avoided and utilized the cylinder reality based shape which is out of roundness. Cylinder bore gets distorted due to high hydrodynamic pressure developed, mechanical and thermal stresses, machine manufacturing inefficiencies, wear phenomenon, clamped force on cylinder head, effects due to tolerances. Oil film thickness would be reduced if 4-lobe bore and elliptical non circular shapes of cylinder are considered, results are more accurate. Mathematically, different cylinder bore deformations were incorporated by using cylinder bore of 3-lobes, 4-lobes,5-lobes even n-lobes. To avoid the computation difficulty, here, elliptical distorted bore is utilized shown in figure.

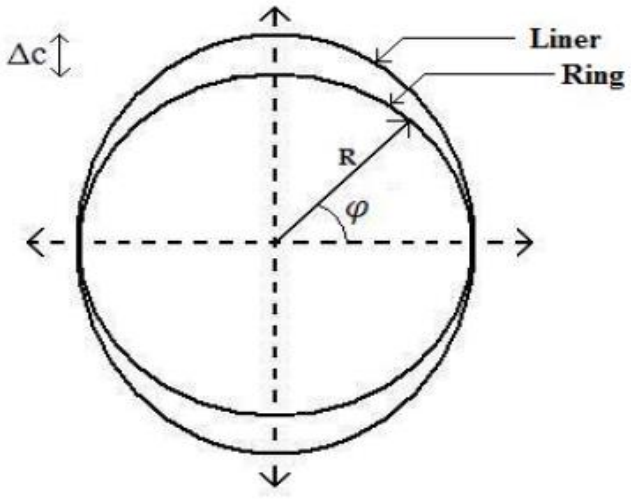

Figure 5.3 Liner Circumferential Deformation [20]

Δc is used for highest value of deformation which change along circumference of cylinder bore, have effects on lubricant film thickness and other tribological parameters. Mathematical relation for this is given as,

$$h_2(y) = R\left\{\frac{1}{\sqrt{1-\left[1-\left(\frac{R}{R+\Delta c}\right)\right]*\sin\varphi}} - 1\right\} \qquad (5.6)$$

$$\varphi = \frac{y}{R} \qquad (5.7)$$

$$0 < y < 2\pi$$

5.6 Ring Hydrodynamic Force

Hydrodynamic force is estimated based on the hydrodynamic pressure generated in the lubricant oil. This hydrodynamic pressure is calculated by Reynolds equation which is integrated on the ring surface to find hydrodynamic force given as,

$$W = \int_0^L \int_0^b p(x,y)dxdy \qquad (5.8)$$

To estimate the correct value of hydrodynamic pressure, radial force balance is required. Condition for radial force balance is given below,

$$FG - W = 0 \qquad (5.9)$$

FG is gas force acts behind the ring in the groove under the assumption that piston only has primary motion. In this case, ring seated in the groove surface that is why gas force is taken which is equal to combustion pressure .This force data for diesel engine used for simulation is given by,

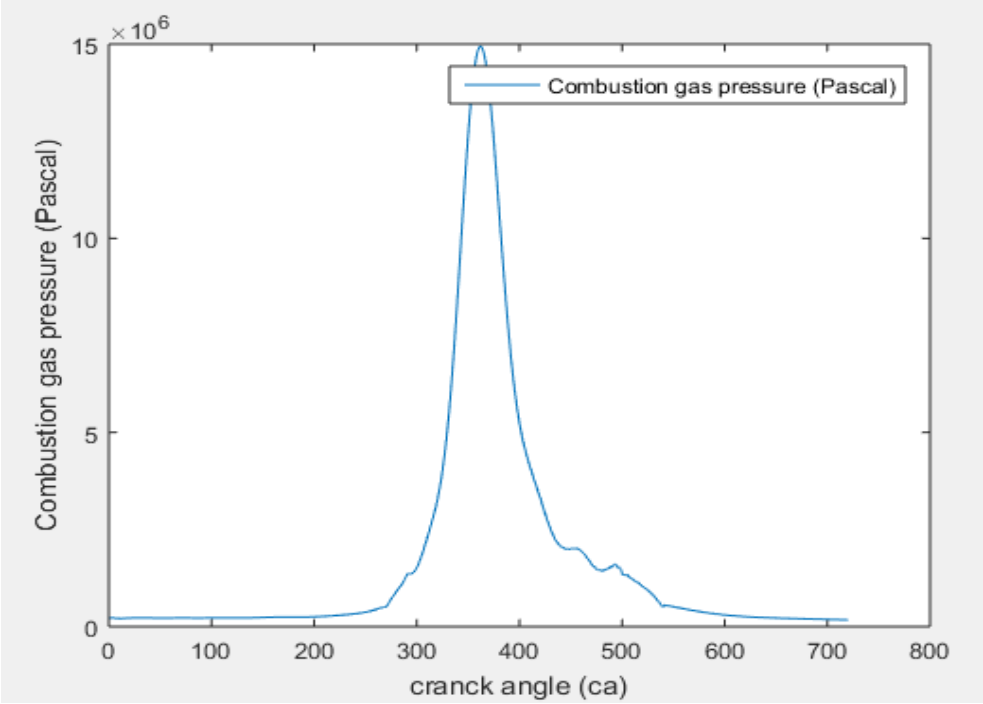

Figure 5.4 Combustion Gas Pressure

5.7 Simulation Procedure

1. Reynolds lubrication model used to determine hydrodynamic pressure based on oil film thickness. This Reynolds equation is discredited explicitly with finite difference scheme (FDM) and solved by successive over relaxation (SOR) method numerically.
2. First of all, lubricant film thickness is calculated at each time step. Initial value of oil film is assumed and new value of h is calculated by using equation (5.11). Hydrodynamic pressure generated in the lubricant is find based on the oil film thickness is solved numerically with Reynolds equation .Other important tribological parameters are calculated based on the hydrodynamic pressure. Reynolds equation is discredited and solved under fully flooded conditions.
3. Based on hydrodynamics pressure, firstly hydrodynamic force W is finds and then respective moment is calculated. Similarly, friction force is estimated based on the viscous shear rate, then moment due to friction force is calculated by integrating on the whole ring surface area.
4. As a result of successful estimation of oil film thickness new value is trialed on the same considering radial position is calculated.
5. Initially h is set equal to minimum film thickness to avoid complexity.
6. Next value of film thickness is updated by the given by,

$$FG - W < 0.00001 \qquad (5.9)$$

$$h_0{}^{(k)}{}_{approx} = \left(\frac{FG}{W}\right)^{\gamma} h_0{}^{(k)}{}_{old} \quad (5.10)$$

$$h_0{}^{(k)}{}_{new} = h_0{}^{(k)}{}_{old} + \lambda_1 \left(h_0{}^{(k)}{}_{approx} - h_0{}^{(k)}{}_{old}\right) \qquad (5.11)$$

$W =$ Hydrodynamic load , $\lambda_1 =$ Under relaxation factor ranges from $0.15 - 0.50$, $FG =$ Gas force , $\gamma =$ Emperical coefficient ranges between 0.1 to 0.2, $k =$ crank angle position

5.8 Friction Force

Friction force is hydrodynamic friction force estimated based on viscous shear effect by integrating shear stress. Shear rate is defined by $\frac{du}{dz}$

$$\tau = \eta \frac{du}{dz} \qquad (5.12)$$

$$u = \left[\frac{z^2 - zh}{2\eta}\right] \frac{dp}{dy} + (U_1 + U_2)\frac{z}{h} + U_2 \quad (5.13)$$

$\eta =$ dynamics viscosity, h is oil film, $\frac{dp}{dy}$ is developed gradient of pressure in circumferential direction, $U2$ presents velocity on ring surface, U is cylinder liner velocity. For the case $U1 = U$ and $U1 = 0$, velocity of fluid in equation (5.13) is given by,

$$u = \left[\frac{z^2 - zh}{2\eta}\right]\frac{dp}{dy} + U\frac{z}{h} + U_2 \qquad (5.14)$$

When velocity component in equation (5.15) is integrated with respect to 'z' then it becomes shear-rate in z direction $\frac{du}{dz}$

$$\frac{du}{dz} = (2z - h)\frac{1}{\eta}\left(\frac{dp}{dy}\right) - \frac{U}{h} \qquad (5.15)$$

$$\frac{du}{dz} = \left(z - \frac{h}{2}\right)\frac{1}{\eta}\left(\frac{dp}{dy}\right) - \frac{U}{h} \qquad (5.16)$$

Considering equation (5.15) and (5.16) into equation (5.12). It becomes,

$$\tau = \eta\left(z - \frac{h}{2}\right)\frac{1}{\eta}\left(\frac{dp}{dy}\right) - \frac{U}{h} \qquad (5.17)$$

$$\tau = \left(z - \frac{h}{2}\right)\left(\frac{dp}{dy}\right) - \frac{U}{h} \qquad (5.18)$$

$$\tau = \left(-\frac{h}{2}\right)\left(\frac{dp}{dy}\right) - \eta\frac{U}{h} \qquad (5.19)$$

Equation (5.20) represents the average shear value on ring surface can be expressed.

$$\tau = \eta\frac{U}{h} - \frac{h}{2}\frac{dp}{dy} \qquad (5.20)$$

$$F_{vis} = \int_0^L \int_0^b \tau \, dxdy$$

$$F_{vis} = \int_0^L \int_0^b \eta\frac{U}{h} - \frac{h}{2}\frac{dp}{dy} \, dxdy \qquad (5.21)$$

5.9 Flow Rate

Lubricant oil flow rate which is available in ring liner region when ring is sliding. This oil flow rate in sliding direction of ring can be estimated.

$$q_x|_{x=xt} = \frac{U\,h_t}{2} - \frac{{h_t}^3}{12\eta}\frac{\partial p}{\partial x}|_{x=x_t} \qquad (5.22)$$

Here subscript x_t indicates the trailing edge location where q_{x2} leave the ring surface.Total flow due to lubricant oil can be found by integratingq_{x2}.

Therefore, total flow rate between ring and liner surfaces at any time can be represented as,

$$Q = \int_0^L q_x \, dy \qquad (5.23)$$

CHAPTER 6

NUMERICAL PROCDURE, NON-DIMESIONALIZATION

6.1 Dimensionless Form of Reynolds Equation

2-D Reynolds equation for steady state case in non-dimensional so variables in equation (6.1) can be written as,

$$h^* = h/c \quad , \qquad x^* = {}^{x}/_{R}$$

$$p^* = {}^{pc^2}/_{6U\eta R} \qquad y^* = {}^{y}/_{L}$$

R Represents the radius of piston in [m], after substituting the given variable and parameters in equation (6.1) gives the new dimensionless form of Reynolds equation is given as,

$$\frac{\partial}{\partial x^*}\left(\frac{h^{*3}}{12}\frac{\partial p^*}{\partial x^*}\right) + \left(\frac{R}{L}\right)^2 \frac{\partial}{\partial y^*}\left(\frac{h^{*3}}{12}\frac{\partial p^*}{\partial y^*}\right) = \frac{\partial h^*}{\partial x^*} \qquad (6.1)$$

6.2 Vogelpohl Parameter

Initially vogelpohl parameter was used in 1930 when it was observed that with the introduction of this parameter numerically accuracy was improved for the solution of Reynolds lubrication model. This is given as,

$$M_v = p^* h^{*1.5} \qquad (6.2)$$

By substituting equation (6.2) Reynolds equation in (6.1) becomes,

$$\frac{\partial^2 M_v}{\partial x^{*2}} + (\frac{R}{L})^2 \frac{\partial^2 M_v}{\partial y^{*2}} = \mathrm{F} M_v + G \qquad (6.3)$$

Equation (6.3) is in non-dimensional form known as vogelpohl equation.
G and F for piston and rings can be written as,

$$F = \frac{0.75 * [\ \left(\frac{\partial h^*}{\partial x^*}\right)^2 + \left(\frac{R}{L}\right)^2 \left(\frac{\partial h^*}{\partial x^*}\right)^2\ ]}{h^{*2}} + \frac{1.5 * [\frac{\partial^2 h^*}{\partial y^{*2}} + \left(\frac{R}{L}\right)^2 \frac{\partial^2 h^*}{\partial y^{*2}}\ ]}{h^*} \qquad (6.4)$$

$$G = \frac{(\frac{\partial h^*}{\partial x^*})}{h^{*1.5}} \qquad (6.5)$$

Vogelpohl parameters assists to solve Reynolds equation easily by simplifying differential operator of order second in x and y direction. Moreover, it does not contain higher value in final form of equation. It is obvious that higher values in equation create truncation error.

6.3 Reynolds Equation Equivalence with Finite Difference

Non-dimensional form of Reynolds model will be discretized by finite difference method so it can be written as,

$$\left(\frac{\partial \mathrm{M_v}}{\partial \mathrm{x}^*}\right) = \quad \left(\frac{(\mathrm{M_{v,i+1}}) - (\mathrm{M_{v,i-1}})}{2\delta \mathrm{x}^*}\right) \qquad (6.6)$$

Here i+1 an i-1 subscript are to be used to denote the position immediate located at front and behind the central node i. deltax described the constant step size between any two nodes. Same type of relation is used for second order $\partial \mathrm{M_v}$. The computation is represented in figure (6.1) given as,

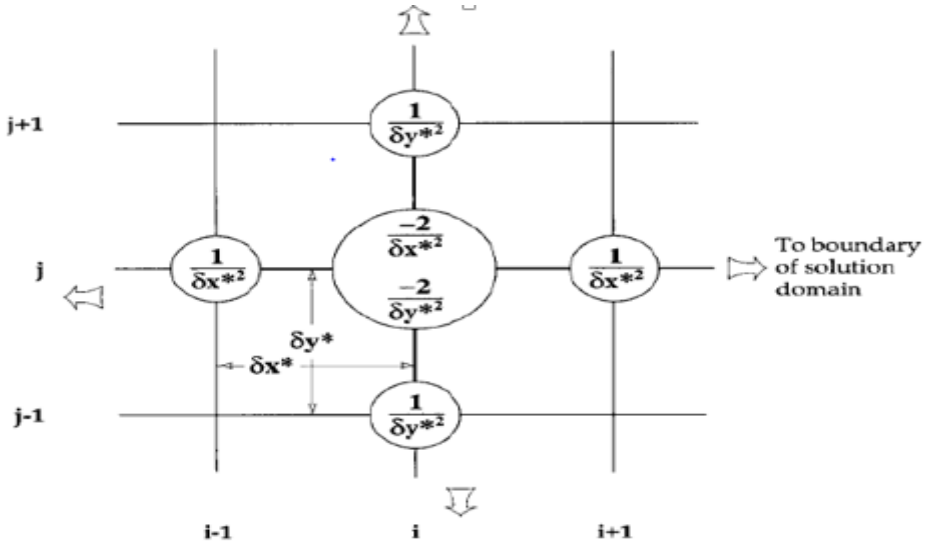

Figure 6.1 Numerical Analysis [20]

It is defined based on the when M_v at i-0.5 is subtracted from M_v at i+0.5r simultanously divided by delta x.

$$\frac{\partial^2 \mathrm{M_v}}{\partial \mathrm{x}^{*2}} = \quad \left(\frac{\left(\frac{\partial \mathrm{M_v}}{\partial \mathrm{x}^*}\right)_{\mathrm{i+0.5}} - \left(\frac{\partial \mathrm{M_v}}{\partial \mathrm{x}^*}\right)_{\mathrm{i-0.5}}}{\delta \mathrm{x}^*}\right) \qquad (6.7)$$

$$\left(\frac{\partial \mathrm{M_v}}{\partial \mathrm{x}^*}\right)_{\mathrm{i+0.5}} = \frac{\mathrm{M_{v,i+1}} - \mathrm{M_v}}{\delta \mathrm{x}^*} \qquad (6.8)$$

$$\left(\frac{\partial \mathrm{M_v}}{\partial \mathrm{x}^*}\right)_{\mathrm{i-0.5}} = \frac{\mathrm{M_v} - \mathrm{M_{v,i-1}}}{\delta \mathrm{x}^*} \qquad (6.9)$$

On substitution of equation into (6.8) becomes,

$$\left(\frac{\partial^2 \mathrm{M_v}}{\partial \mathrm{x}^{*2}}\right)_i = \quad \left(\frac{(\mathrm{M_{v,i+1}} - \mathrm{M_{v,i-1}} - 2\mathrm{M_{v,i}})}{\delta \mathrm{x}^{*2}}\right) \qquad (6.10)$$

Above is found from by finite difference $\frac{\partial^2 M_v}{\partial x^{*2}} + \frac{\partial^2 M_v}{\partial y^{*2}}$ equivalency of M_v in two direction in x and y-axes. Along y-axis, at second position nodal position variable is introduced i.e, 'j' parameters. Two expressions are similar $\frac{\partial^2 M_v}{\partial y^{*2}}$ and $\frac{\partial M_v}{\partial y^*}$. In x-axis but have but the difference is

that i is replaced by j. Coefficient of M_v at ith node and its neighboring node is needed from Reynolds equation and resulted in finite difference operator denoted as calculated molecules given in figure (6.1).

Finite difference operator is easily used computationally and does not produce any problem when calculating at boundary nodes. In the case when finite difference operator is situated at the boundary nodes important arrangements are needed outside the boundary with boundary nodes. In case of ring and liner surfaces, we have a defined region on which our computational solution is defined. Two term in the form of F and G defined by finite difference method may be included to from an equivalent form of Reynolds equation. The new form of equation may by rearranged for expression M_v as,

$$\mathrm{M_{v,i,j}} = \frac{\mathrm{C1}*\left[\left(\mathrm{M_{v,i+1,j}}+\mathrm{M_{v,i-1,j}}\right)\right]+\left(\frac{\mathrm{R}}{\mathrm{L}}\right)^2\mathrm{C_2}*\left(\mathrm{M_{v,i,j+1}}+\mathrm{M_{v,i,j-1}}\right)-\mathrm{G_{i,j}}}{2\mathrm{C_1}+2\mathrm{C_2}+\mathrm{F_{i,j}}} \qquad (6.11)$$

Where

These relation become the basis of the solution of discretized form of Reynolds equation to solve by FDM .It gives the required values M_v at a given node.

$$\mathrm{C_2} = \frac{1}{\delta \mathrm{y}^{*2}},$$

$$\mathrm{C_1} = \frac{1}{\delta \mathrm{x}^{*2}}$$

For piston ring surface the boundary conditions are needed that 'p*' or M_v are zero at the edges of cylinder ring surface additionally that cavitation can happen to avoid negative hydrodynamic pressures happening inside these surfaces. The extension of 'x*' is between 0-360 degree point for the cylinder ring. The run of 'y*' is from -0.5 to +0.5 if the mid-line of cylinder ring is chosen as a datum. A space of the cylinder ring where symmetry can be relaxed to include either half of the cylinder ring region varies from y* = to y* = 0.5 or total piston skirt area.

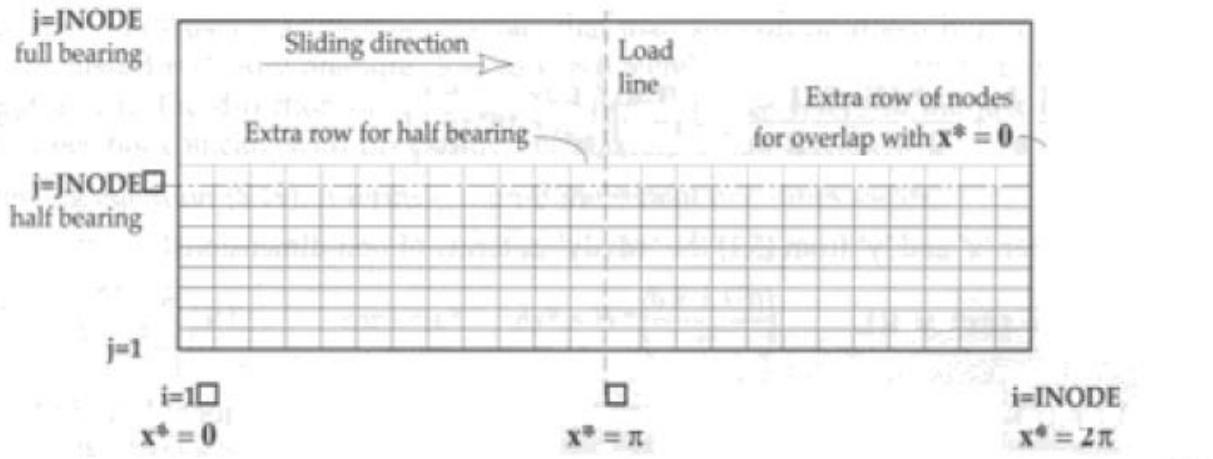

Figure 6.2 Computational Grid on Ring Surface [20]

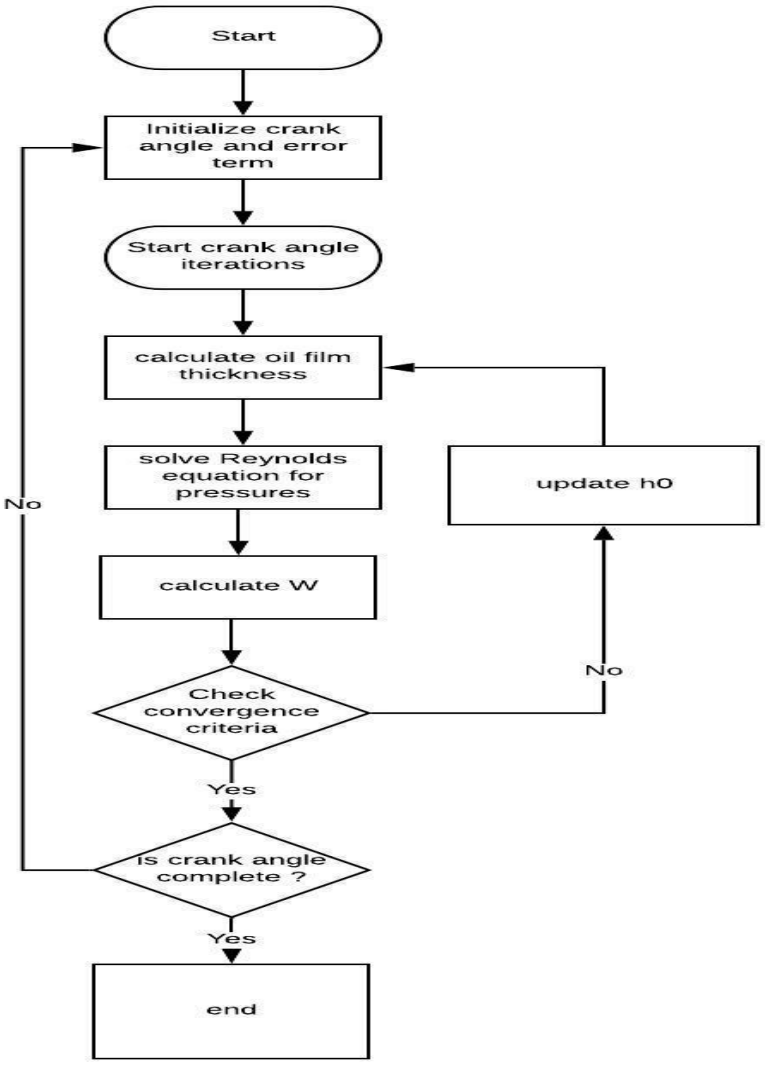

Figure 6.3 Flow Chart for Hydrodynamic Pressure Computation

CHAPTER 7

RESULTS AND DISCUSSIONS

7.1 Combustion Gas Pressure and Groove Pressure

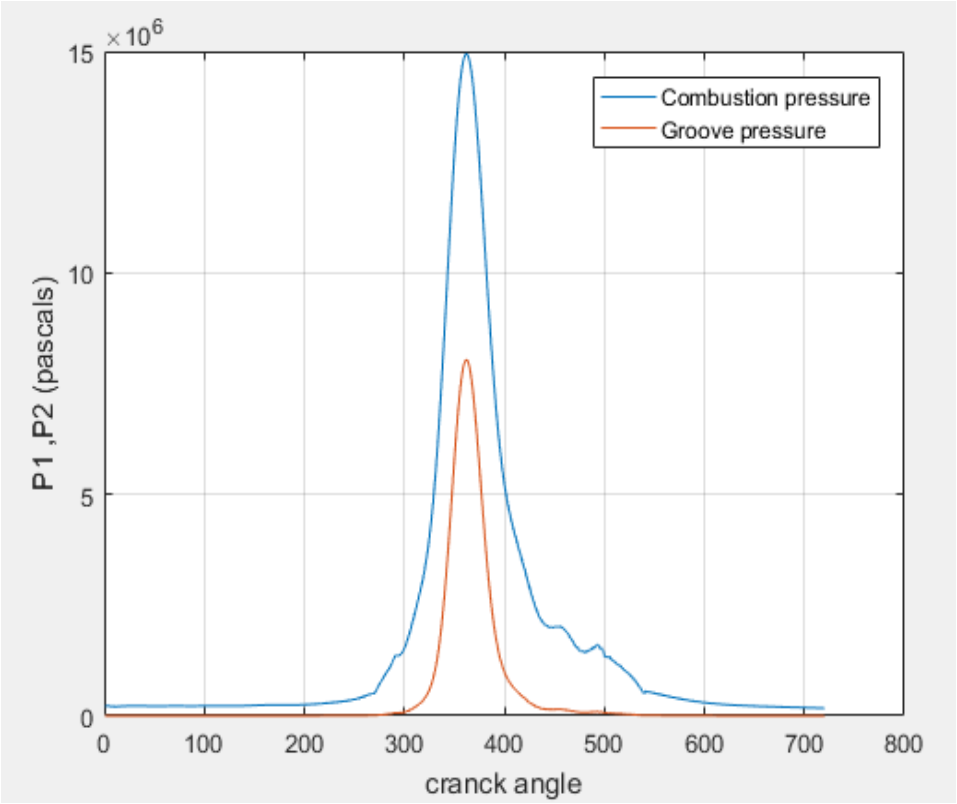

Figure 7.1 Combustion Gas Pressure and Groove Pressure

First groove pressure is measured numerically by gas flow model based on the cylinder pressure which is less than combustion pressure. In above figure (7.1) it is shown measured gas pressure ‘‘P2’’ in first groove region. Mostly pressure in first groove increases during downward stroke and decreases during upward stroke. At crank angle 360 during power stroke, maximum gas pressure developed in the second groove of value 7Mpa. At engine speed 2000 rpm and maximum ring groove clearance 3e-5m, peak value of groove pressure remains less than combustion pressure during engine cycle. Because only first compression ring is included so pressure in the second land directly faces crank case pressure which is equal to the 1 atm pressure. Under high speed/low load condition, second groove pressure decreases, while groove pressure increases when clearance increases to the maximum value of 3e-5m. It is shown in the figure that pressure in the first groove is always much less than combustion chamber pressure because it has peak value 7 Mpa while combustion chamber has peak pressure 15Mpa.

7.2 Ring Groove Reaction Force

Ring axial position within the groove is decided based on the ring groove clearance and imbalance of surface forces. These surface forces are consisted of piston inertial force, gas pressure force and friction force. Ring groove relative motion is determined for one complete engine cycle. Maximum value of axial clearance used in the groove is 3e-5m. In figure (7.2) it is shown that during the intake stroke, ring sits on top groove flank side. During intake stroke, when piston crosses the middle of the stroke the ring reached to the lower flank of groove. In diesel engine, due to high gas pressure force on ring groove upper surface keep sitting on the lower flank of the groove for most of the time then at the start of the exhaust stroke when ring inertial force dominates then ring moves to the upper side of groove and remains seated until one engine cycle completed. Ring movement within the groove is defined by the sign of changing reaction force. Changing sign of reaction force decides ring position in the groove. When ring starts moving from the groove upper or lower surface within the groove. When ring is either stuck on the upper flank of groove or lower flank of groove.

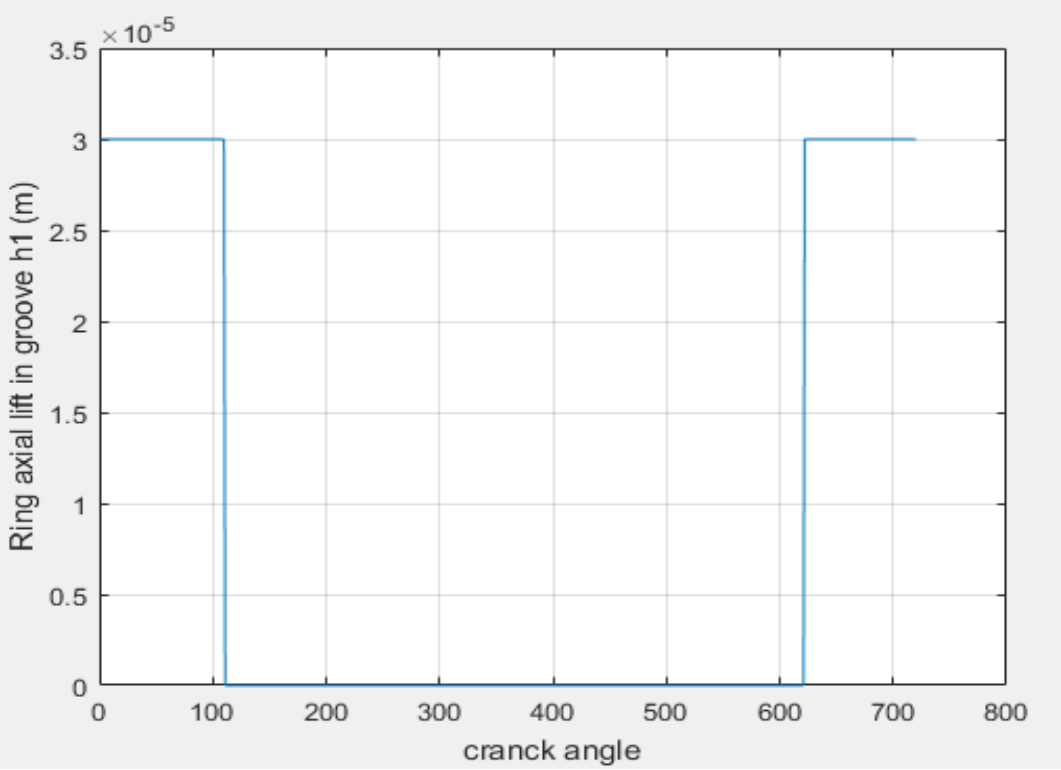

Figure 7.2 Ring Groove Reaction Force

7.3 Ring Surface Forces

Figure (7.3) shows the effect of inertial force, upper gas pressure force, lower gas pressure, friction force when engine operates at 2000 rpm at maximum clearance of 3e-5m. Among all the force, gas pressure has maximum in magnitude as compared to other forces. In this case, inertial force is very small in magnitude which cannot resists ring moving downward during intake stroke. Friction force always acts against ring motion. Similarly, inertial effect of ring is very minute as compared to gas pressure force. High upper gas pressure force is dominated throughout the engine cycle that is why ring remain seated almost all the time. As long as the summation of surface forces keep positive, so ring remains seated on the lower groove flank.

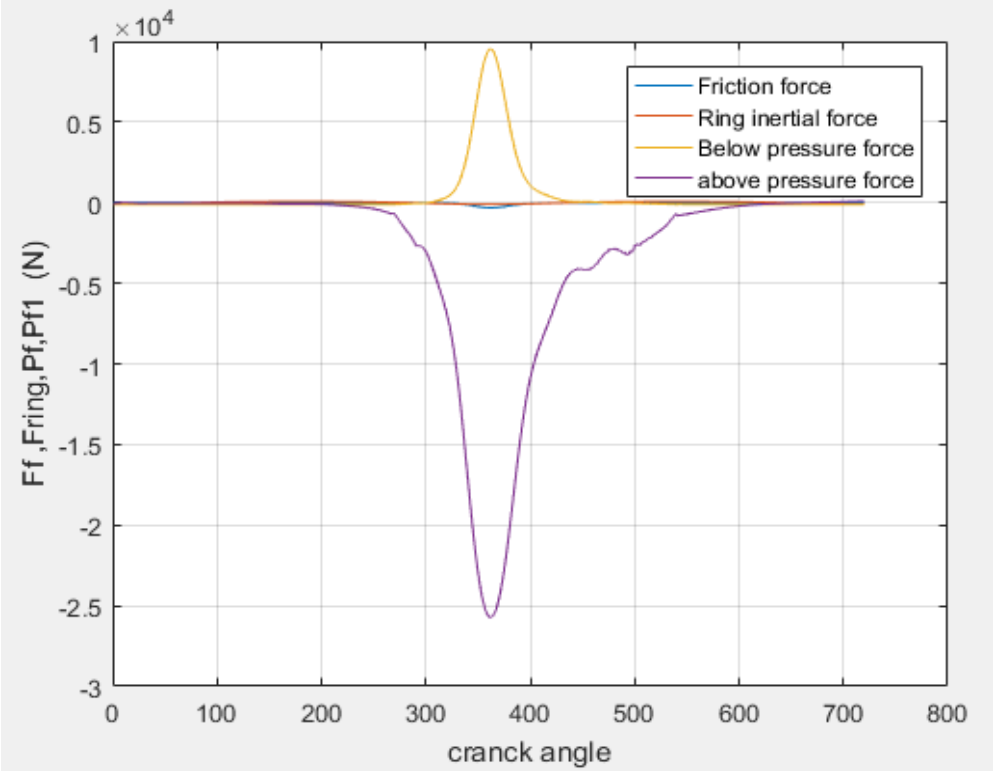

Figure 7.3 Forces Acting on Ring Surfaces

7.4 Gas Flow Rate Within First Groove

Leakage of blow-by gases from combustion chamber side to crankcase side takes place through ring and groove side clearance change. In the figure (7.4) it is shown that gas flows is very small through groove and ring clearances when gas leaks from combustion side crosses the first groove side clearance and flow toward the second land .At the start of intake stroke, ring seals completely gas flow with the upper groove flank than after some crank angles ring starts moving toward lower groove flank which provides the blow-by gases a clearance path through which blow-by

gases leaks from combustion chamber side to crankcase side. Maximum value of gas blow-by reached -1.6e-4 kg/s during power stroke when high pressurized gas gets a chance to flow toward crank case. It was observed that some spikes show behavior on the positive side during few crank angles its means gas back blow happens due to high pressure difference between crankcase to combustion chamber.

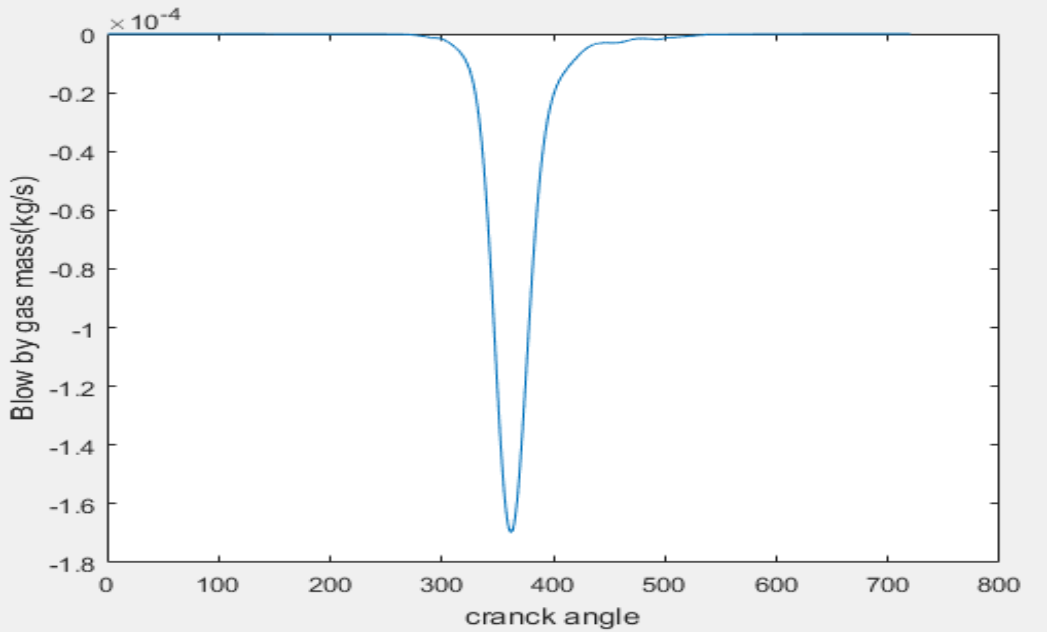

Figure 7.4 Gas flow Rate within First Groove

7.5 Minimum Oil Film Thickness without Piston Tilt Effect

Minimum oil film thickness is plotted for a complete engine cycle. From figure (7.5) .It is shown that at the start of intake stroke, Piston cyclic velocity increases oil film thickness start rising. When piston reaches middle of the intake stroke, proper hydrodynamic regime is developed then minimum oil film thickness reaches its peak value more than 2.75e-7m. After mid of stroke as piston moves toward BDC, due to cyclic velocity of piston decreases oil film decreases up to its minimum value. During compression stroke, during to increase in gas force and friction force which let the shift of load to the cylinder side and film thickness does not reach its maximum value again. In compression stroke, film thickness rises again, however, the lubricant regime occurs rigid hydrodynamic regime. During power stroke, due to high gas force backside the ring causes the higher hydrodynamic pressure on ring face to maintain radial balance. As a result, load bearing capacity increases and oil film thickness decreases.

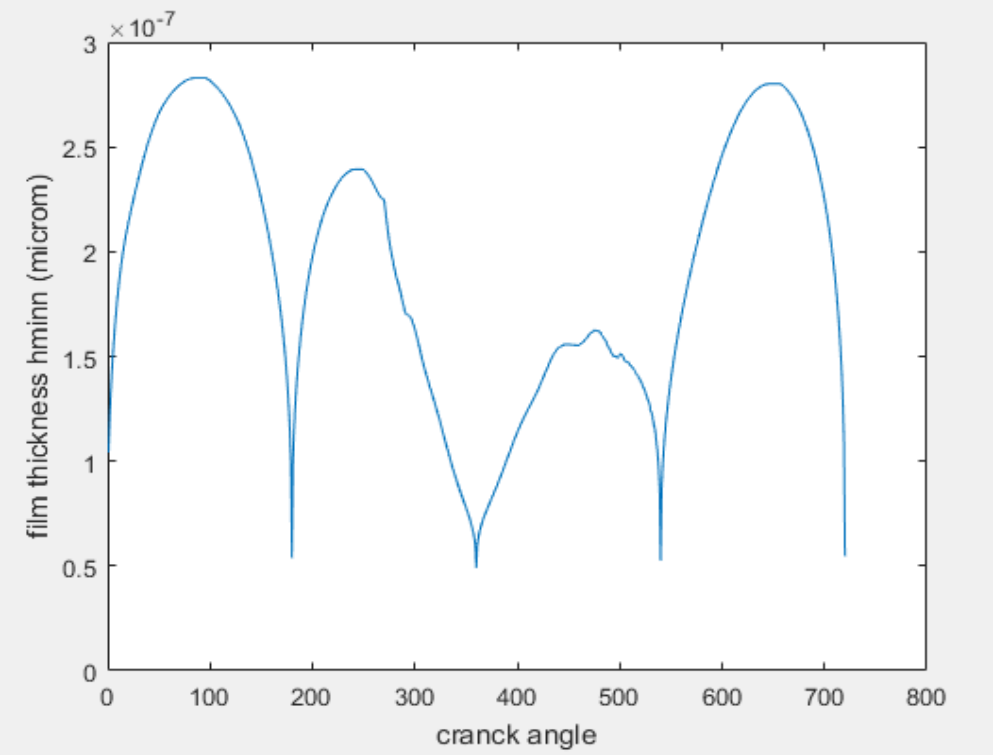

Figure 7.5 Minimum Oil Film Thickness Without Piston Tilt Effect

At last in exhaust stroke/expansion stroke, again film thickness shoots up to its maximum value because combustion pressure decreases which causes the decrease in groove gas pressure behind the ring while radial balance required minimum hydrodynamic pressure to be developed in front of the ring , as a result minimum oil film thickness decreases. It is always made sure that radial balance maintains during complete engine cycle. Minimum value of oil film was noted during power stroke at 360 degree crank angle where its value is 0.5e-7.

7.6 Hydrodynamic Lubrication Pressure between Ring and Liner without Piston Tilt

Hydrodynamic pressure developed in oil film indicates loading bearing capacity. High value of gas force back surface of the ring is responsible for ring radial balance within ring liner interface. Figure (7.6) shows the trend of hydrodynamic pressure during one complete engine cycle. During intake stroke, pressure start increases because gas pressure is low at start due to which minimum load bearing capacity is required in front of the ring. On the other hand, piston slow down near TDC as there is great chance of boundary lubrication because of which very small hydrodynamic pressure developed. Trend in figure (7.6) shows continues increase in hydrodynamic pressure during compression stroke which shows that high gas combustion pressure behind the ring requires a high hydrodynamic pressure in front of the ring. During power stroke, hydrodynamic pressure reaches its peak value at about 6.3e7 Pas.

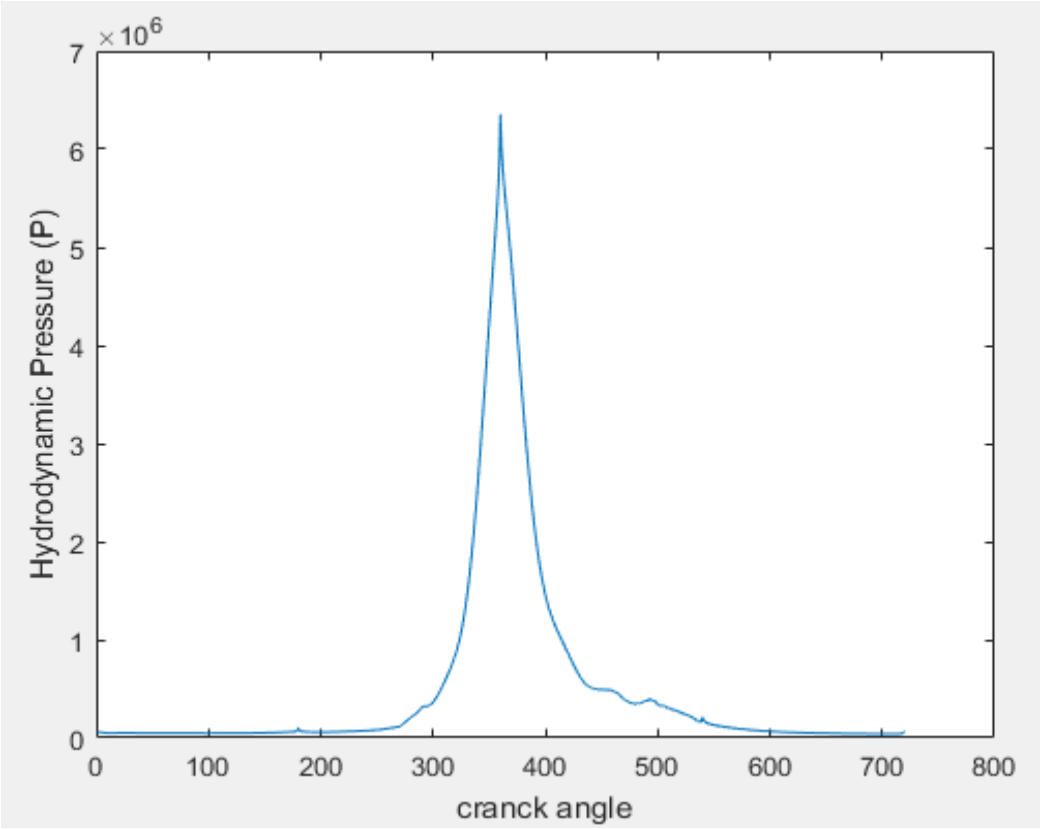

Figure 7.6 Hydrodynamic Lubrication Pressure between Ring and Liner without Piston Tilt

This increase in hydrodynamic pressure is because of high gas pressure behind the ring which requires a high hydrodynamic pressure in front of the ring to ensure radial balance. During exhaust stroke, hydrodynamic pressure decreases, because load bearing capacity decreases which require a low hydrodynamic pressure in front of the ring.

7.7 Hydrodynamic Pressure for Piston Skirt Lubrication with Piston Tilt effect

Figure (7.7) shows hydrodynamic pressure developed within film thickness by considering the effect of piston angular motion (tilt motion) on ring dynamics. Piston tilt motion have crucial effect on ring lubrication as shown in figure (7.7). During intake stroke, hydrodynamic pressure start increases but this increase in pressure in not much prominent this is because piston is eccentric and piston tilt motion has very little effect. During compression stroke, tilt motion increases which increases the load bearing capacity as a result hydrodynamic pressure increases. But this increase in hydrodynamic pressure in not much prominent. During power stroke, hydrodynamic pressure increases with additional effect of piston tilt motion and hydrodynamic pressure reaches up to the maximum value. During exhaust stroke, tilt motion shows its effect as a result hydrodynamic pressure increases but again this increase in hydrodynamic pressure is not

very high. Tilt motion have minor contribution in the ring lubrication, but this effect is significant to understand the lubrication theory of piston-ring interaction.

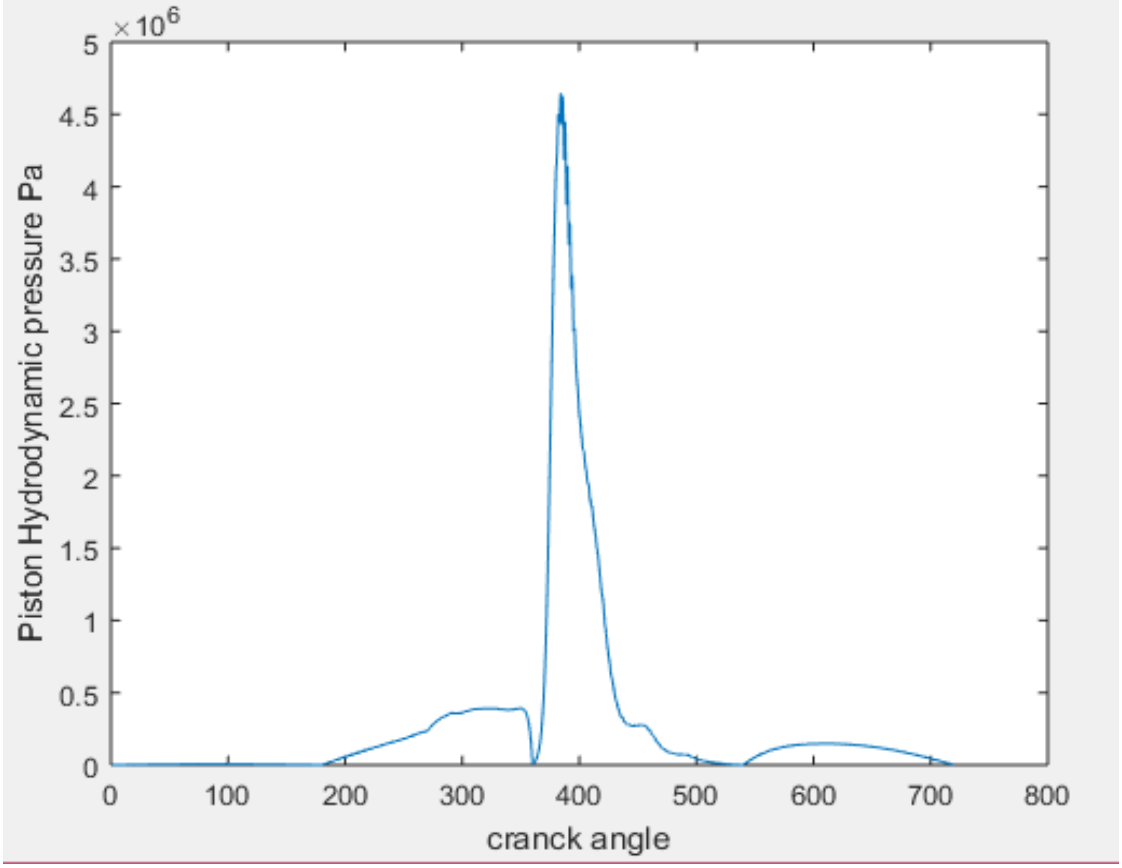

Figure 7.7 Hydrodynamic Pressure of Ring and liner with Piston Tilt

7.8 Ring Hydrodynamic Friction Force without Piston Tilt

Fluid friction force generated when hydrodynamic regime developed during complete engine cycle. Friction force enhance the power loss, energy dissipation. During induction stroke, piston move from TDC to BDC due to low gas pressure and low hydrodynamics pressure results in low magnitude of friction force. During compression stroke, Due to high values of gas combustion pressure, hydrodynamics pressure and lubricant shear results in higher value of friction force. At the start and end of intake stroke, compression stroke, power stroke and exhaust stroke, friction force shows minimum value, because of slow variations of piston cyclic velocity. During compression stroke and power stroke, due to maximum changes in film thickness, hydrodynamic pressure and combustion gas pressure have cumulative in increase in friction force. During exhaust stroke, change in decrease in friction force is occurred due to decrease in gas pressure and hydrodynamic pressure.

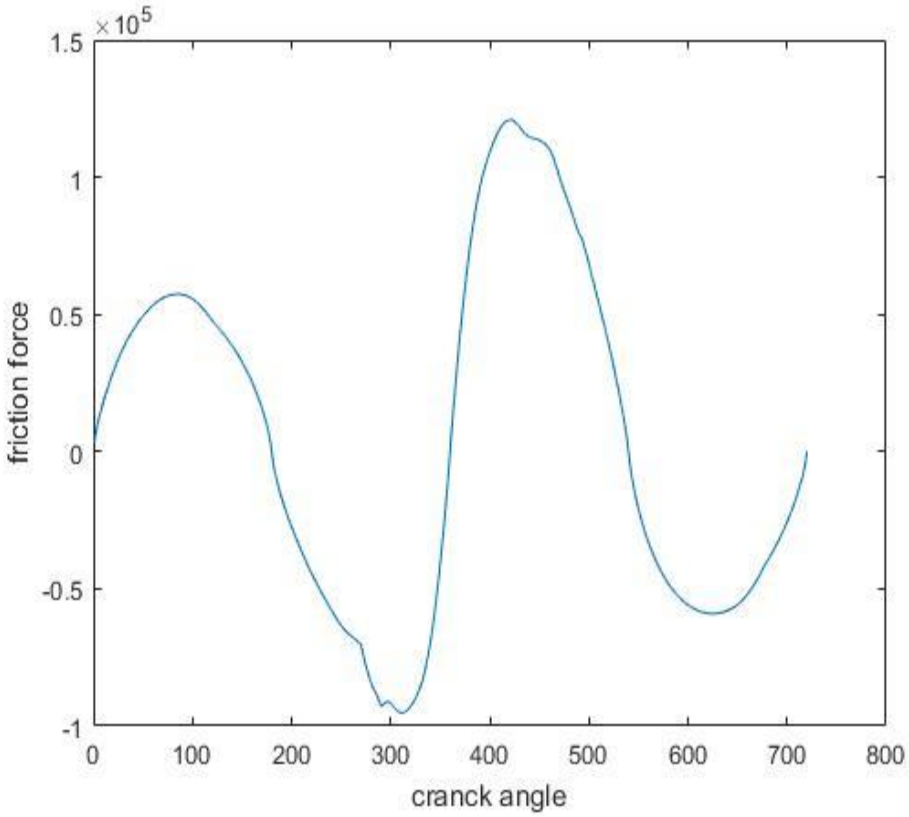

Figure 7.8 Hydrodynamic Friction Force of Ring and Liner Lubrication without Piston Tilt

7.9 Ring Hydrodynamic Friction Force with Piston Tilt

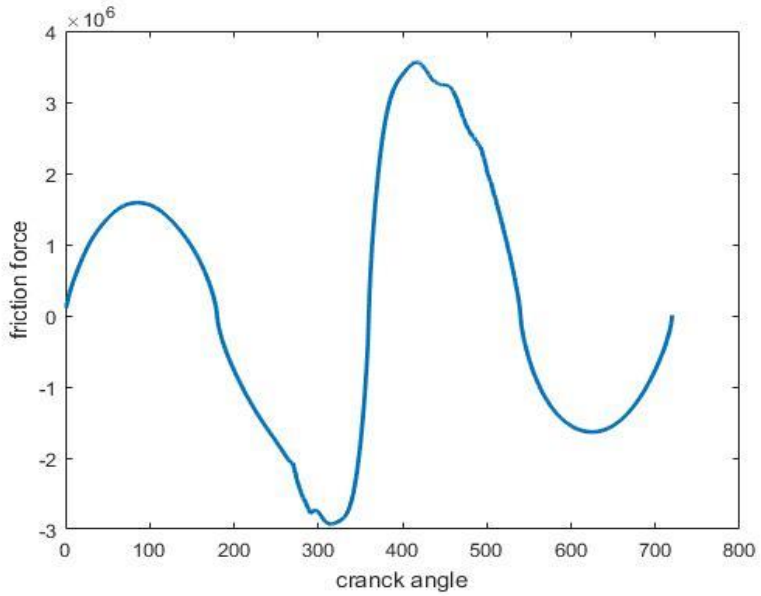

Figure 7.9 Hydrodynamic Friction Force of Ring and Liner Lubrication without Piston Tilt

It is shown in the figure (7.9) above, piston tilt plays important role in the increase in friction force. During intake stroke, as tilt effect of piston secondary motion increases which results in higher magnitude of friction force. During compression stroke, as the tilt value increases combined with higher values of gas pressure, hydrodynamic pressure causes increase in magnitude of friction force. During power stroke, under high gas combustion pressure and hydrodynamic pressure and piston tilt value results in increase of friction force. In exhaust stroke, when gas combustion pressure and hydrodynamic pressure decreases with tilt effect result in low friction force in magnitude. From figure (7.9) it is clear that overall effect of tilt motion dominates throughout the engine cycle.

7.10 Piston Tilt without Ring Hydrodynamic Force Effect

Figure (7.10) shows the piston tilt motion without considering the effect of ring hydrodynamic force. Initially piston is placed at the center of cylinder. During an engine cycle, piston shows secondary motion is represented in term of tilt motion. During intake stroke, tilt start to increases due to transverse imbalance of side forces and moments in radial direction. Under high value of inertial forces of piston and wrist pin the hydrodynamic pressure decreases which results in lateral tilt motion .During compression stroke, under high value of inertial effect piston tilt reaches it maximum value. Then piston tilt start to decrease during power stroke and tilt shows negative which presents piston motion in thrust side. During exhaust stroke, piston again moves to the anti-thrust side which means piston is moving back to its original position.

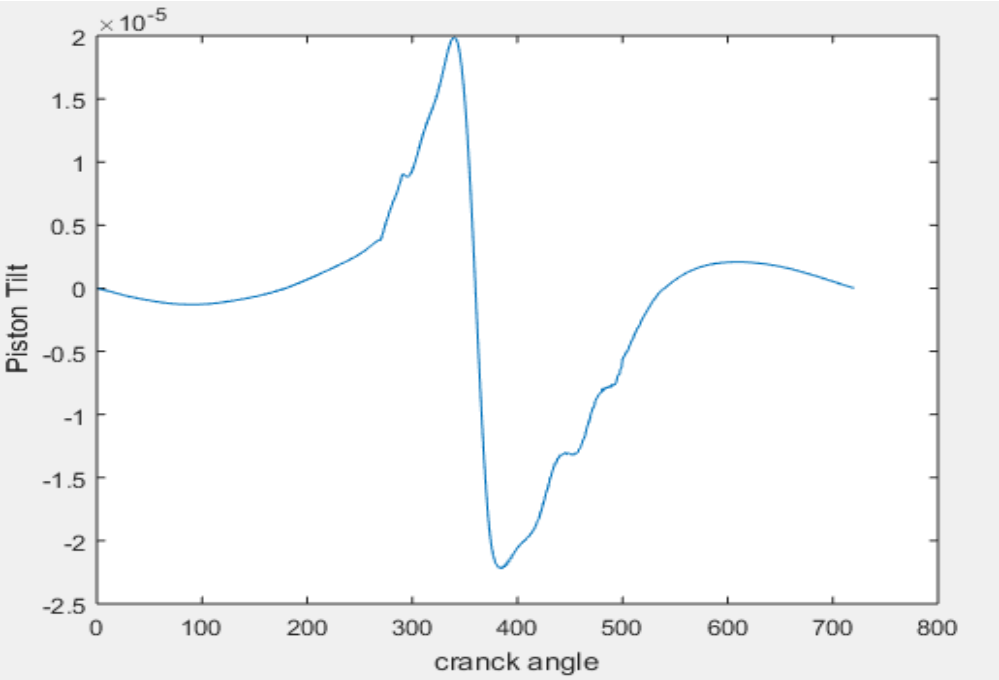

Figure 7.10 Piston Tilt without Ring Hydrodynamic Force Effect

7.11 Piston Tilt with Ring Hydrodynamic Pressure Effect

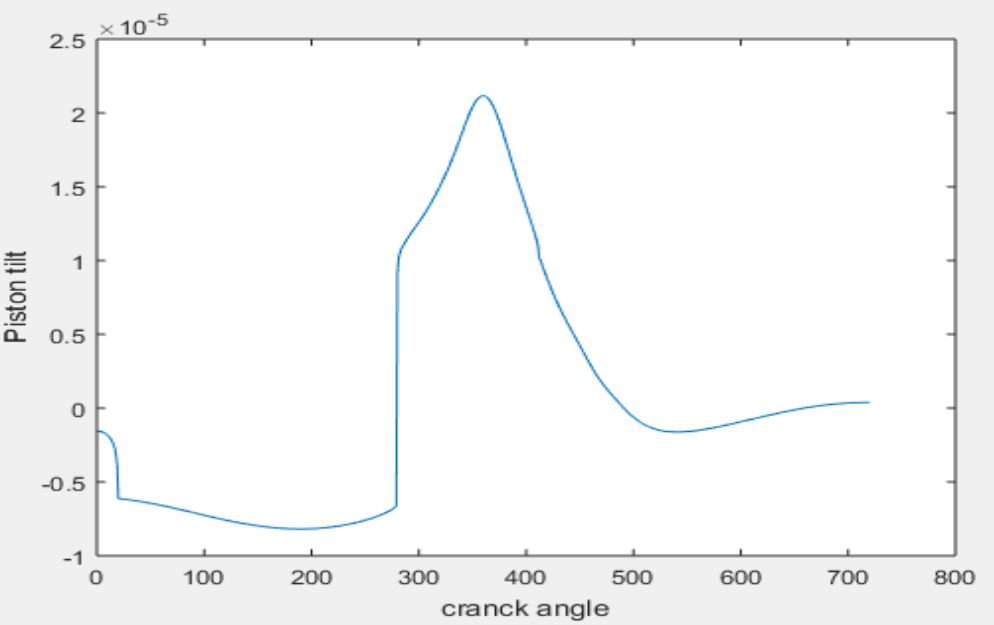

Figure 7.11 Piston Tilt with Ring Hydrodynamic Force Effect

Figure (7.11) shows that poison tilt motion is predicted when ring hydrodynamic pressure is included. When intake stroke starts, piston tilt shows negative value which means piston starts moving to the negative thrust side. This is because of high ring friction force and ring hydrodynamic pressure force. During compression stroke, piston remained inclined toward negative thrust side which means higher hydrodynamic pressure develops on the opposite thrust side. At 290 degree crank angle, piston moves toward thrust side due to higher thrust force on piston crown. During power stroke, higher hydrodynamic pressure develops along the higher gas force their occurred a shift its tilt motion. Just after the start of the power stroke, piston tilt is at maximum value 2e-5radians then it decreases. At exhaust stroke, piston tilt almost remains smooth this happened because in the balance of piston inertial forces and skirt face forces due to ring friction force and ring hydrodynamic force.

CHAPTER 8

COCLUSIONS AND FUTURE WORK

8.1 CONCLUSIONS

Some important conclusions in this research work has been drawn which are given below,

- In ring axial motion, it was concluded that gas flow is very sensitive to ring-groove side clearance.
- Piston tilt motion enhanced the ring hydrodynamic friction between ring-liner interfaces.
- Piston tilt motion increases the overall friction losses due to which oil consumption increases.
- At high value of viscosity, shear rate increases due to which friction loss increases.
- Connecting rod dynamics improves the piston lateral force balance. Due to which proper piston hydrodynamic lubrication developed.
- At big value of clearance in piston radial direction, at thrust side and anti-thrust side disturb the proper generation of hydrodynamic pressure.
- At high value of speed, proper hydrodynamic film thickness generated within ring-liner region.
- Distorted cylinder liner results in lower magnitude of oil film in circumferential cylinder side, which results in enhanced oil consumption due to oil leakage toward combustion chamber side burns lubricant oil and friction losses and power losses increases.
- Parabolic type of ring face is more suitable design for proper lubrication phenomena.
- At high value of piston speed, proper hydrodynamic regime developed between ring-liner region which keeps the ring and liner surfaces apart as a result avoid the direct contact.

8.2 Future Work

- The present analysis may be expand for the whole piston ring pack.
- In this work, parametric study is not done. Better understanding may be built if analysis is performed by changing ring radial clearances, RPM, loading conditions.
- Effect of Elastohydrodynamic lubrication, viscous heating, solid coating layer, starvation, thermal expansion are not included in the present study. Inclusion of these effects would make the analysis more realistic.
- Gas flow rate may be measured with experimental base to better estimate the deviation with simulation based result.

REFERENCES

[1] Comfort, “An Introduction to Heavy-Duty Diesel Engine Frictional Losses and Lubricant Properties Affecting Fuel Economy - Part 1,” Dec. 2004.

[2] Pavel Novotny, Vaclav Pistek, Lubomir Drapal, David Svı ´da and Tomas Devera , ‘‘Efficient approach for solution of the mechanical losses of the piston ring pack,’’ 22 May 2013.

[3] Nasha Wei, James Xi Gu and Fengshou Gu,’’ An Investigation into the Acoustic Emissions of Internal Combustion Engines with Modelling and Wavelet Package Analysis for Monitoring Lubrication Conditions,’’ 16 February 2019.

[4] S. H. Mansouri and V. W. Wong, “Effects of piston design parameters on piston secondary motion and skirt-liner friction, ‘‘ Proceedings of the Institution of Mechanical Engineers, Part J: Journal of Engineering Tribology, vol. 219, no. 6, Article ID J03604,pp.435–449,2005.

[5] J. Zhang and Y. Meng, “Direct observation of cavitation phenomenon and hydrodynamic lubrication analysis of textured surfaces,”TribologyLetters,vol.46,no.2,pp.147–158,2012.

[6] F. M. Meng, Y. Y. Zhang, Y. Z. Hu, and H. Wang, “Thermoplastic-hydrodynamic lubrication analysis of piston skirt considering oil film inertia effect,” Tribology International,vol.40,no. 7,pp.1089–1099,2007.

[7] Y.-C. Tan and Z. M. Ripin, “Technique to determine instantaneous piston skirt friction during piston slap,” Tribology International,vol. 74,pp.145–153,2014.

[8] F. M. Meng, X. F. Wang, T. T. Li, and Y. P. Chen, “Influence of cylinder liner vibration on lateral motion and tribological behaviors for piston in internal combustion engine,” Proceedings of the Institution of Mechanical Engineers, Part J: Journal of Engineering Tribology, vol. 229, no.2,pp. 151–167,2015.

[9] P.Obert, T.M¨uller and D.Bartel,“The influence of oil supply and cylinder liner temperature on friction, wear and scuffing behavior of piston ring cylinder liner contacts a new model test,”Tribology International,vol.94,pp.306–314,2016.

[10] R. Mazouzi, A. Kellaci, and A. Karas, “Effects of piston design parameters on skirt-liner dynamic behavior,” Industrial Lubrication and Tribology, vol.68,no.2,pp. 250–258,2016.

[11] Fang, X. Meng, and Y. Xie, “A piston tribodynamic model with deterministic consideration of skirt surface grooves,” TribologyInternational,vol.110,pp.232–251,2017.

[12] Z. Zhang, Y. Xie, X. Zhang, and X. Meng, "Analysis of piston secondary motion considering the variation in the system inertia," Proceedings of the Institution of Mechanical Engineers, Part D: Journal of Automobile Engineering, vol. 223, no. 4, pp. 549–563,2009.

[13] X.MengandY.Xie,"A new numerical analysis for piston skirt liner system lubrication considering the effects of connecting rodinertia,"TribologyInternational,vol.47,pp.235–243,2012

[14] X. Meng, L. Ning, Y. Xie, and V. W. Wong, "Effects of the connecting-rod-related design parameters on the piston dynamics and the skirt-liner lubrication," Proceedings of the Institution of Mechanical Engineers,PartD:Journal of Automobile Engineering,vol.227,no.6,pp.885–898,2013

[15] L.Ning, X.Meng, and Y.Xie ," Incorporation of deformation in a lubrication analysis for a automotive piston skirt-liner system," Proceedings of the Institution of Mechanical Engineers, Part J: Journal of Engineering Tribology, vol. 227, no. 6, pp. 654–670, 2013.

[16] L. McMillan Simon C. Tung and Michael, "Automotive tribology overview of current advances and challenges for the future", Tribology International vol. 37, pp. 517-536, 2004.

[17] Andrew W. Batchelor and Gwidon W. Stachowiak, Engineering Tribology, Elsevier Butterworth-Heinemann, 2005, pp.103-112.

[18] Edward P. Becker, "Trends In Tribological Materials and Engine Technology", Tribology International, vol. 37, pp. 569-575, 2004.

[19] Jaana Tamminen, Peter and Sandstrom, "Piston ring tribology a Literature survey", VTT Research Notes, No. 2178, pp. 8, 2002.

[20] Malik M A, Ali U, Adnan Q S and Riaz M "Modeling of piston top ring lubrication by considering cylinder out-of-roundness in initial engine start up," London: International Congress on Mechanical Engineering, 2010.

[21] Liang Liu, "Modeling the Performance of the Piston Ring-Pack with Consideration of Non-Axisymmetric Characteristics of the Power Cylinder System in Internal Combustion Engines" Massachusetts Institute of Technology(MIT), pp.15-23, 2005.

[22] S. L. Moore and G.M. Hamilton, "The Lubrication of Piston Rings First Paper Measurement of the Oil-Film Thickness Between the Piston Rings and Liner of a Small Diesel Engine" IMechE, vol. 188, pp. 253-261, 1974.

[23] O. Reynolds, On the Theory of Lubrication and its Application to Mr. Beauchamp Tower's Experiments Including an Experimental Determination of the Viscosity of Olive Oil, Phil. Trans., Roy. Soc. London, Vol. 177 (i), 1886, pp. 157-234.

[24] G.M. Hamilton and S. L. Moore, “Comparison between Measured and Calculated Thicknesses of the Oil-Film Lubricating Piston Ring”, IMechE, vol 188, pp. 262-268, 1974.

[25] Mufti R.A., Priest M., Chittenden R.J.: Analysis of piston assembly friction using the indicated mean effective pressure experimental method to validate mathematical models. Proc. Instn Mech. Engrs, Part D: Journal of Automobile Engineering, 222(8): pp.1441-1457, 2008.

[26] Keith, T.Jr., and Yang, Q.“Two-Dimensional Piston Ring Lubrication—Part I: Rigid Ring and Liner Solution,”, Trib. Trans., vol. 39, pp. 3, 1996

[27] M. Hiruma, H. Yoshida, S. Furhama et K.Shin "Effect of piston ring movement upon oil consumption". JSAE, Mars 1983.

[28] C.A.Amann "Engineering the spark-Ignition Engine- the Piston-Ring-cylinder wall interface". SAE 885056, 1988.

[29] Bernard Hamrock and Mohsen Esfahanian, “ On the Hydrodynamic Lubrication Analysis of Piston Rings”, Lubrication sciences 10-4, pp. 265-286, August 1998

[30] Kurbet S N and Kumar R K "Finite element modeling of piston-ring dynamics and blow-by estimation in a four-cylinder diesel engine," Proceedings of the Institution of Mechanical Engineers Part D Journal of Automobile Engineering,pp. 1405-1414, 2007

[31] Ruddy B L, Dowson D and Economous P N "The prediction of gas pressures within the ring packs of large bore diesel engines," Jour. Mechan. Eng. Science 23,vol. 6,pp 295-304, 1981.

[32] Keribar R, Dursunkaya Z and Flemming M F "An integrated model of ring pack," Ricardo-ITI, Inc.,Westmont, IL 60559, 1981.

[33] Namazian M and Heywood J B "Flow in the piston-cylinder-ring crevices of a spark-ignition engine: effect on hydrocarbon emissions, efficiency and power," SAE Paper 820088, 1982.

[34] Furuhama S, Masaru H "Piston ring motion and its influence on engine tribology," SAE Paper 790860, 1980.

[35] Liu Y, Chen W. W and Zhu D" An elastohydrodynamic lubrication model for coated surfaces in point contacts," Journal of Tribology, vol. 129, pp. 509-516, 2007.

[36] Tian T, Noordzij L B, Wong V W and Heywood J B "Modeling piston-ring dynamics,blow-by, and ring twist effects," Journal of Engineering for Gas Turbines & Power, Vol. 120,pp 843854,1998a.

[37] Liu Y and Tian T "Development and application of ring-pack model integrating global and local processes. Part 1, gas pressure and dynamic behavior of piston ring pack," SAE Int. Engines,pp. 1927-1939,2017.

[38] Petris C D, Giglio V, Police G "A mathematical model or the calculation of blow-by flow and oil consumption depending on ring dynamic .Part I: gas flows, oil scraping and ring pack dynamic," SAE Paper 941940.

[39] Tian T, Rabute R, Wong V W and Heywood J B "Effects of piston ring dynamics on ring groove wear and oil consumption in a diesel engine," SAE Paper 970835, 1997.

[40] Tian and Liang L "Development and applications of an analytical tool for piston ring design," Powertrain & Fluid Systems Conference & Exhibition, Pennsylvania USA Pittsburgh,2003.

[41] Smith E H ,M-T M and Isherrington "A three-dimensional analysis of piston ringlubrication Part 1: Modeling," IMechE,pp 1-14, September 1995.

[42] Dowson D, Ruddy B.L and Economou P.N "The elastohydrodynamic lubrication of piston pings," Proceeding Royal Society London, 1983.

CERTIFICATE OF COMPLETENESS

It is hereby certified that the dissertation submitted by NS Jamal Ahmed , Reg No. **00000119730**, Titled: ***Modeling and Simulation of 1stRing Dynamics in High Torque Low-Speed Diesel Engine*** has been checked/reviewed and its contents are complete in all respects.

Supervisor's Name: **Dr. Raja Amer Azim** Signature: _____

Date: _____